

Predicting long-term monthly electricity demand under future climatic and socioeconomic changes using data-driven methods: A case study of Hong Kong

Sheng Liu^{a,*}, Aaron Zeng^{b,*}, Kevin Lau^{c,d,e}, Chao Ren^f, Pak-wai Chan^g, Edward Ng^{a,c,d}

^a School of Architecture, The Chinese University of Hong Kong, New Territories, Hong Kong

^b Lab of Data Science, United Technologies, Pudong New District, Shanghai, PR China

^c Institute of Future Cities, The Chinese University of Hong Kong, New Territories, Hong Kong

^d Institute of Environment, Energy and Sustainability, The Chinese University of Hong Kong, New Territories, Hong Kong

^e CUHK Jockey Club Institute of Ageing, The Chinese University of Hong Kong, New Territories, Hong Kong

^f Faculty of Architecture, The University of Hong Kong, Hong Kong Island, Hong Kong

^g Hong Kong Observatory, Kowloon, Hong Kong

ARTICLE INFO

Keywords:

Long-term prediction
Electricity demand
Climate change
Data-driven methods
Machine learning methods

ABSTRACT

Data-driven methods, such as artificial neural networks (ANNs), support vector regression (SVM), Gaussian process regression (GPR), multiple linear regression (MLR), decision trees (DTs), and gradient boosting decision trees (GBDTs), are the most popular and advanced methods for energy demand prediction. However, these methods have not been cross compared to analyze their performances for long-term energy demand predictions. Therefore, this paper aims to identify the best method among these data-driven methods for quantifying the impacts of climatic and socioeconomic changes on future long-term monthly electricity demand in Hong Kong. First, historical 40-year climatic, socioeconomic, and electricity consumption data are used to train and validate these models. Second, different representation concentration pathway (RCP) scenarios and three percentiles of 24 global circulation model outputs are adopted as future climatic changes, while five shared socioeconomic pathways are considered for future socioeconomic uncertainties. The results show that the GBDT method provides the best accuracy, generalization ability, and time-series stability, while ANN method exhibits the lowest accuracy and lower generalization ability. The monthly electricity demands in Hong Kong under the RCP8.5–2090 s scenario are predicted to increase by up to 89.40 % and 54.34 % in the residential and commercial sectors, respectively, when compared with 2018 levels.

1. Introduction

1.1. Background

Since the heating and cooling energy demands are significantly affected by outdoor temperature increases (Andrić, Koc, & Al-Ghamdi, 2019), the relationship between energy consumption and climate change has aroused worldwide concerns in energy management and planning projects (Ahmed, Muttaqi, & Agalgaonkar, 2012; Moazami, Nik, Carlucci, & Geving, 2019). Based on a global projection study (Santamouris, 2016) of the average cooling energy demand in 2050, it is estimated that there will be significant increases by 750 % and 275 % for residential and commercial buildings, respectively, due to future climate

change and socioeconomic development. Especially in China, the number of cooling degree days (CDDs) in 2050 could increase by up to 150 % compared with 2005 under the high emissions scenario (You et al., 2014), and the national electricity demand could grow by approximately 58.6 % from 2020 to 2050 (Mei, Li, Suo, Ma, & Lv, 2020). Since increasing temperatures will alter cooling and heating demand patterns, considerable net increases in energy consumption would most likely occur in areas with high cooling demands (Li, Yang, & Lam, 2012), i.e., tropical and subtropical areas. In subtropical Hong Kong, the building stock consumes more than 90 % of the city's electricity and contributes 60 % of greenhouse gas (GHG) emissions. Among the different sectors, the commercial and residential sectors accounted for 66 % and 27 % of electricity consumption, respectively, in 2018

* Corresponding authors at: School of Architecture, Lee Shau Kee Architecture Building, The Chinese University of Hong Kong, New Territories, Hong Kong.
E-mail addresses: sheng.liu@link.cuhk.edu.hk (S. Liu), zeng.building@foxmail.com (A. Zeng).

<https://doi.org/10.1016/j.scs.2021.102936>

Received 28 October 2020; Received in revised form 23 February 2021; Accepted 10 April 2021

Available online 15 April 2021

2210-6707/© 2021 Elsevier Ltd. All rights reserved.

Table 1
Summary of the literature published after 2015 that has forecasted long-term annual or monthly electricity demand.

Reference	Predication model	Main independent variables	Demand type and temporal scale	Level	Location
(Pérez-García & Moral-Carcedo, 2016)	Regression/econometrics and index decomposition analysis.	GDP, sectoral share of GDP, population	Annual electricity demand till 2030	National	Spain
(Torrini, Souza, Cyrino Oliveira, & Moreira Pessanha, 2016)	Fuzzy logic approach	GDP, population growth	Annual electricity consumption until 2030	National	Brazil
(Günay, 2016)	ANN	GDP, population, inflation percentage, unemployment percentage, average summer temperature, average winter temperature	Annual gross electricity demand until 2028	National	Turkey
(Liang et al., 2016)	MLR, Ridge Regression, Extreme Learning Machine(ELM) hybrid forecasting model	GDP, population, energy policy constraints	Annual electricity demand until 2020	National	China
(Trotter et al., 2016)	MLR	GDP, population, HDDs, CDDs, hours of daylight, calendar effects	Annual electricity demand until 2100	National	Brazil
(Ang et al., 2017)	Time-series approach and decomposition approach	Monthly average temperature, time trend, seasonal variation (holidays)	Electricity consumption per month 2011–2015	City	Singapore and Hong Kong
(Kaboli et al., 2017)	optimized gene expression programming, ANN, SVM, adaptive neuro-fuzzy inference system	GDP, population, import, export	Annual electricity consumption until 2030	National	ASEAN-5 countries
(Li, 2018)	MLR	Monthly CDD, relative humidity, wind speed, rainy days	Monthly electricity consumption 2005–2016	National	Singapore
(Hamedmoghadam et al., 2018)	Deep Neural Networks and ANN	GDP, population, precipitation, average temperature, average minimum temperature, and average maximum temperature	1 to 24 months ahead monthly electricity demand	National	Australia
(da Silva, Cyrino Oliveira, & Souza, 2019)	Bottom-up approach with linear hierarchical models	Production by process, specific electricity consumption (SEC) by process, value added of the sector, electricity price	Annual electricity consumption for pulp and paper industry until 2050	National	Brazil
(Fan et al., 2019)	MLR	HDDs, CDDs, rainfall and sunshine, Per capita GDP, electricity price, urbanization rate, technology progress	Electricity demand growth by 2100	National	China
(Toktarova et al., 2019)	MLR	Temperature, GDP, population, industrial production, day duration.	Annual electricity demand until 2035	National	Sweden, Iran, Finland
(Chabouni, Belarbi, & Benhassine, 2020)	MLR	CDDs, HDDs, Fixed and movable seasonality variables	Electricity demand without a case study	National	Algeria
(He et al., 2019)	Hybrid Simulated Annealing (SA)-Chicken Swarm Optimization (CSO) algorithm	GDP, population, energy structure, industrial structure and urbanization	Annual electricity demand until 2035	National	China
(Kaytez et al., 2015)	Hybrid model with least-square SVM, ANN and regression models	Gross electricity generation, population, installed capacity, import, export and total subscribership	Net electricity consumption until 2022	National	Turkey
(Zheng et al., 2020)	MLR	GDP, population, electricity price, CDDs and Heating Degree Days (HDDs)	Electricity consumption until the 2080s	City	Guangzhou (China)

(Electrical & Mechanical Services Department, 2021). Moreover, electricity consumption per capita in the residential and commercial building sectors grew significantly from 4.4 GJ in 1989 to 19.8 GJ in 2018 (Electrical & Mechanical Services Department, 2021). Coincidentally, anthropogenic climate change has resulted in a continuous increase in temperature records in Hong Kong, with an average increase rate of 0.17 °C per decade from 1989 to 2018 (Hong Kong Observatory, 2019). Apart from weather-induced consumption, total electricity consumption has increased considerably over the long-term due to steady economic and population growth with continuous improvements of living standards (Morakinyo et al., 2019). Given this reality, as time progresses, electricity consumption, especially space cooling demand in the future, could inevitably increase due to future exacerbated climate change and further socioeconomic development.

At present, long-term energy prediction (normally longer than one year) is a subject of widespread interest among researchers and energy policy makers who are concerned with the accuracy and robustness of prediction models (Khuntia, Rueda, & van der Meijden, 2016). Accurate predictions of energy demand play a vital role in energy planning and policy formulation. Inaccurate predictions, i.e., underestimations or overestimations, of energy demand lead to potential outages or unnecessary excess capacity. For example, Hobbs (1999) reported that a 1 % decrease in the mean absolute percentage error (MAPE) in the prediction

model could save 10,000 MW h of energy and 1.6 \$ million in a specific fiscal year. In addition to energy planning and management, predicting reliable energy use patterns under different future climate and socioeconomic scenarios could provide a useful reference for policy makers regarding climate change mitigation strategies and energy saving plans over time (Isaac & van Vuuren, 2009). Therefore, accurate and reliable long-term energy demand predictions which incorporate future climate change and socioeconomic uncertainties could avoid costly mistakes and help policy-makers understand climate change and socioeconomic impacts.

1.2. Literature review

Predicting a city's future electricity demand in the long term is highly uncertain and complex, as it depends on various factors, including climate change and socioeconomic development, such as gross domestic product (GDP) and population growth, as well as technological developments (Ghalekhondabi, Ardjmand, Weckman, & Young, 2017). As far as long-term energy demand predictions with annual/monthly variables are concerned, there are several factors, such as climatic, technological, demographic and socioeconomic variables that affect future energy demand growth (Xia, Wang, & McMenemy, 2010). The pre-2015 literature regarding forecasting long-term electricity demand

is well documented in two review studies (Ghalekhondabi et al., 2017; Lindberg, Seljom, Madsen, Fischer, & Korpås, 2019), and more recent studies after 2015 are presented in Table 1. The commonly used demographic and socioeconomic variables in the previous literature included GDP, population, and electricity price, while the climatic variables that normally include CDDs and technological development were rarely considered. However, separate consideration of socioeconomic variables and climate change variables has usually been limited in most previous studies (see Table 1). Only a few recent studies (Fan, Hu, & Zhang, 2019; Günay, 2016; Trotter et al., 2016; Zheng, Huang, Zhou, & Zhu, 2020) have combined the uncertainties in demographic and socioeconomic variables and future climate change variables. For instance, (Trotter et al., 2016) presented a probabilistic long-term electricity demand forecasting study for Brazil that incorporated climatic, demographic, and economic uncertainties. However, they only considered the future climatic outputs from one general circulation model (GCM); thus, the possible biases from different GCMs were ignored in their study. Günay (Günay, 2016) used several climatic and economic variables to forecast the annual electricity demand in Turkey, but the future climatic uncertainties from GCMs were not incorporated in this study. Fan et al., 2019 proposed a linear regression model for 30 provinces in China and incorporated climate variables such as heating degree days (HDDs), CDDs, rainfall and sunshine and socioeconomic variables, such as per capita GDP, electricity price, and urbanization rate. A similar approach and dataset were adopted by Zeng et al. (Zheng et al., 2020) to explore the influence of climate change on electricity consumption in Guangzhou, China.

Although these previous studies on long-term energy demand predictions used multiple climatic and socioeconomic variables, they only considered one or several GCMs. However, apart from the uncertainty in different climate change scenarios, the intermodel divergence among different GCMs could be the main source of uncertainty when projecting the future climate and should be considered as future climatic uncertainties (Zhai & Helman, 2019). These previous studies (Fan et al., 2019; Günay, 2016; Trotter et al., 2016; Zheng et al., 2020) have not addressed future climatic projection uncertainties among the different GCMs. Moreover, dry-bulb temperatures, CDDs and heating degree hours (HDDs) are some commonly used climatic variables, while other important climatic variables, such as wet-bulb temperatures, solar radiation and enthalpy, which could be significant for the thermal comfort and energy use patterns in subtropical climates, are usually ignored. In subtropical cities such as Hong Kong, which has hot and humid summers during which the relative humidity can often be higher than 90 %, even up to 100 % (Hong Kong Observatory, 2019); the local residents prefer to use a “hybrid” strategy, i.e., they switch on air-conditioner and close windows only when the indoor thermal environment is intolerable for them, to cool residential buildings (Liu, Kwok, Lau, Ouyang, & Ng, 2020). As air-conditioner usage in “hybrid” buildings is influenced by the occupants’ window-opening behaviors and indoor thermal comfort, humidity and solar radiation could be potential factors that influence air conditioning usage (Luo, Cao, Damiens, Lin, & Zhu, 2015). To fill this gap, in this study, both climatic and socioeconomic variables, including dry-bulb temperatures, wet-bulb temperatures, solar radiation, enthalpy, GDPs and population size, are considered as potential variables. Future climatic and socioeconomic data are obtained by down-scaling the climatic outputs from 24 GCMs from the Coupled Model Intercomparison Project Phase 5 (CMIP5) database and socioeconomic outputs from the shared socioeconomic pathways (SSPs) database.

Apart from comprehensively considering possible climatic and socioeconomic uncertainties, a well-performing forecasting model is important for the accuracy of long-term energy predictions. The state-of-art forecasting techniques that are applied to long-term energy predictions are summarized below. Previously, traditional forecasting models, such as linear regression models (Aranda, Ferreira, Mainar-Toledo, Scarpellini, & Llera Sastresa, 2012; Fang & Lahdelma, 2016; Li, 2018; Trotter et al., 2016; Zheng et al., 2020), econometrics

(Pérez-García & Moral-Carcedo, 2016; Vu, Muttaqi, & Agalgaonkar, 2015), and time series (Ang, Wang, & Ma, 2017; García-Ascanio & Maté, 2010), have been widely used for long-term energy prediction due to their simplicity of application and explanation of results. However, traditional linear regression models have limitations in rejecting insignificant explanatory variables and addressing the problem of multicollinearity (Zheng et al., 2020). In contrast, machine learning methods can handle nonlinearity among variables and do not require adoption of a particular functional relationship between inputs and outputs (Kon-tokosta & Tull, 2017). In light of this, some researchers have shed light on the applicability of machine learning methods for energy demand predictions (Ghalekhondabi et al., 2017; Ghods & Kalantar, 2011). Especially, machine learning methods are widely used and compared for short-term or middle-term energy predictions; these include artificial neural networks (ANNs) (Luo, Oyedele, Ajayi, & Akinade, 2020; Seyedzadeh et al., 2019), support vector machines (SVMs) (Kavaklioglu, 2011; Shao, Wang, Bu, Chen, & Wang, 2020; Zhong, Wang, Jia, Mu, & Lv, 2019), decision trees (DTs) (Chen et al., 2019) or gradient boosting decision trees (GBDTs) (Robinson et al., 2017; Touzani, Granderson, & Fernandes, 2018), genetic algorithms (GAs) (Assareh, Behrang, Assari, & Ghanbarzadeh, 2010; Yu, Wei, & Wang, 2012), Gaussian process regression (GPR) (Sangrody, Zhou, & Tutun, 2018; Yang, Li, Li, & Qu, 2018) and some hybrid models (He, Wang, Guang, & Zhao, 2020; Liang, Niu, Cao, & Hong, 2016). Due to the difficulties in quantifying forecasting uncertainties and data availability, a limited number of studies have used machine learning methods for long-term energy predictions. Among the different machine learning methods, the ANN has been the most popular machine learning method for long-term energy predictions. For instance, Günay (Günay, 2016) adopted the ANN model to predict electricity demand in Turkey until 2028 and found that the ANN model exhibited higher accuracy than the traditional linear regression model. In a similar study, Kankal et al. (Kankal, Akpınar, Kömürcü, & Özşahin, 2011) found that the ANN model could estimate the energy consumption for Turkey better than regression models by using socioeconomic and demographic variables. Kandananond (Kandananond, 2011) predicted electricity demand in Thailand and found that the ANN method shows better mean absolute percentage errors than the multiple linear regression (MLR) and autoregressive integrated moving average methods. In contrast, a few studies have compared the performance of ANNs with other machine learning methods for long-term energy demand predictions. For instance, Kaytez et al. (Kaytez, Taplamacioglu, Cam, & Hardalac, 2015) reported that SVM achieved better results than the ANN and MLR models for Turkey’s annual electricity consumption predictions. Hamedmoghadam et al. (Hamedmoghadam, Joorabloo, & Jalili, 2018) used ANNs and deep neural networks to predict Australia’s long-term electricity demand and stated that deep neural networks exhibited better performance than ANNs. Based on import, export and socioeconomic datasets, Kaboli et al. (Kaboli, Fallahpour, Selvaraj, & Rahim, 2017) found that optimized gene expression programming provided higher accuracy for annual electrical energy predictions than other artificial intelligence methods, such as ANN, SVM and other linear and quadratic models. Furthermore, Jang et al. (Jang, Byon, Jahani, & Cetin, 2020) demonstrated that a new probabilistic modeling approach that used the nonhomogeneous generalized extreme value distribution provided better fits for predicting the density of long-term daily peak demand than a trend-based approach using linear and quadratic functions. On the other hand, some problems, such as overfitting and local optima, were found in machine learning models (Fouquier, Robert, Suard, Stéphan, & Jay, 2013). For example, Deng, Fannon, & Eckelman, 2018 applied six regressions and machine learning techniques to compare their prediction performances. The researchers found that linear regression models exhibit better performance than machine learning methods for forecasting peak loads of energy use.

A single algorithm cannot outperform all others; different methods have their own appropriate application contexts and could be the best possible approach in energy prediction modeling as a function of

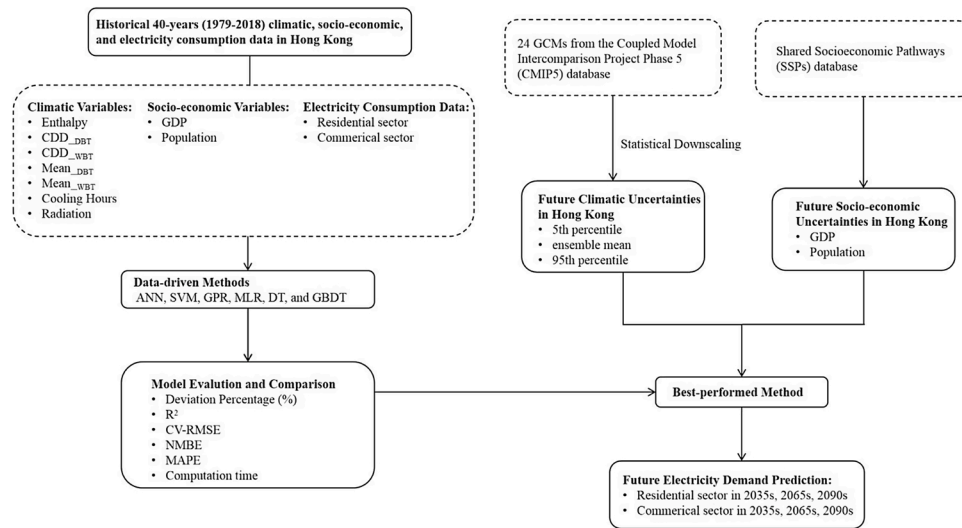


Fig. 1. Flowchart of the proposed methodology for the long-term electricity prediction framework.

multiple input variables. In addition, the selection of input variables determines the performance of algorithms for a given dataset (Ghods & Kalantar, 2011). However, in the long-term energy prediction field, the

existing literature has usually focused on comparisons between an individual machine learning method and traditional regression models or ANNs with limited input variables. Performance comparisons among

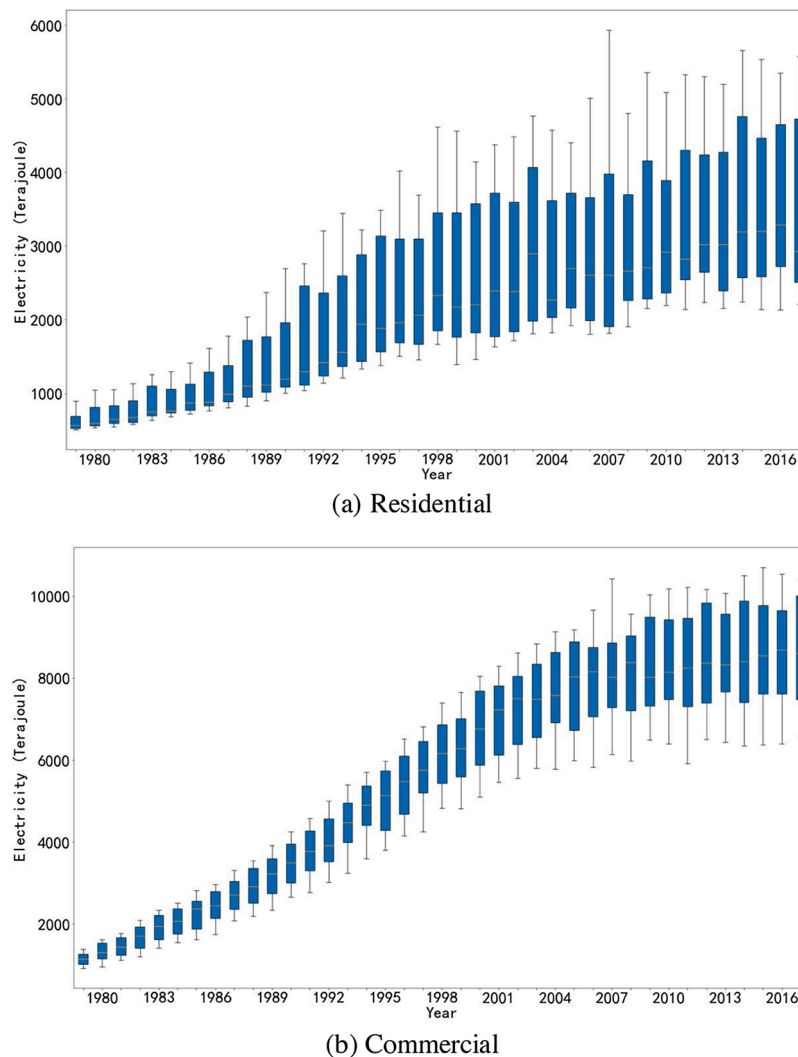


Fig. 2. Boxplots of historical monthly electricity consumption in the Hong Kong residential sector (a) and commercial sector (b).

various data-driven methods for long-term energy prediction are still nonexistent. Thus, there is an opportunity to study the performance comparison of various data-driven algorithms, not only the commonly used ANN and MLR but also the state-of-the-art SVM, GPR, DT, and GBDT methods, for long-term energy predictions based on feasible climatic and socioeconomic datasets.

1.3. Research gaps and contributions

In summary, previous works have usually used a limited number of climatic and socioeconomic variables to train the models and have not considered the full range of future climatic uncertainties from different GCMs. In addition, the existing literature does not systematically compare the performance of various state-of-the-art machine learning methods, such as SVM, GPR, DT, and GBDT, for long-term energy prediction based on feasible climatic and socioeconomic datasets. Taking the subtropical city of Hong Kong as a case study, this study aims to compare the superiority or limitations of different data-driven algorithms, which include ANN, SVM, GPR, MLR, DT, and GBDT, for long-term energy predictions and to identify the best method among these data-driven methods to quantify the impacts of climatic and socioeconomic changes on future long-term monthly electricity demands at the city scale. In this study, the different data-driven models use both climatic and socioeconomic variables, including dry-bulb temperatures, wet-bulb temperatures, solar radiation, enthalpy, GDP and population size, as potential variables, and the intermodel biases among the different GCMs will be considered.

Therefore, the main contributions of this study are twofold. First, in the field of long-term energy prediction, performance comparisons of the popular data-driven algorithms using climatic and socioeconomic variables and selecting the best-performing and applicable model are presumably of great worldwide interest under global climate and socioeconomic changes. Second, a reliable and well-performing model that can be used to assess the long-term impacts of future climate change and socioeconomic development on electricity demand is urgently needed and would be valuable for Hong Kong energy policymakers when they address energy planning and management and climate change mitigation strategies.

2. Material and methods

The framework of the methodology carried out in this paper is presented in Fig. 1. To investigate the impacts of climatic and socioeconomic changes on long-term electricity demand, historical 40-year climatic, socioeconomic, and electricity consumption data in Hong Kong are first collected and were used to train and validate the ANN, SVM, GPR, MLR, DT, and GBDT models. Then, future climatic and socioeconomic uncertainties are used as inputs for the best-performing model to predict future electricity demand. The detailed data collection, theory and algorithm of data-driven methods, model validation and error calculation are discussed in this section.

2.1. Data preparation

2.1.1. Historical and future meteorological data

Data on climatic variables and monthly electricity consumption are collected to analyze the relationship between the changing climate and electricity consumption over the past 40 years. The monthly electricity consumption data of the residential and commercial sectors from 1979 to 2018 were obtained from the [Census and Statistics Department of Hong Kong \(2019a\)](#). The monthly electricity consumption of the residential and commercial sectors from 1979 to 2018 are plotted in Fig. 2. The data were provided by the two electricity suppliers in Hong Kong: China Light and Power (CLP Power) Hong Kong Limited and the Hong Kong Electric (HKE) Company, Limited. Historical hourly meteorological data from 1979 to 2018 were acquired from the Hong Kong

Observatory (HKO) headquarters station. The HKO headquarters weather station is a representative ground-level urban station located in Tsim Sha Tsui, which is a densely developed station in the urban center of Hong Kong ([Cheung & Hart, 2014](#)). More importantly, key meteorological variables, including dry-bulb air temperatures (T_d), wet-bulb temperatures (T_w), and relative humidity (RH), have been recorded at this meteorological station since 1970. Global solar radiation (SR) data were acquired from the King's Park (KP) station, which is also located in the TST area and is 1.2 km from the HKO headquarters station ([Lau, Ng, Chan, & Ho, 2017](#)).

As Hong Kong is located in a coastal region and experiences many hot and humid summers where the air enthalpy is closely related to the cooling load, the conventional cooling degree days metric that is based on dry-bulb temperature (CDD_{DBT}) may not be a suitable indicator for determining energy demands for space cooling ([Guan, 2009](#)). In this study, cooling degree days that are based on wet-bulb temperatures (CDD_{WBT}) are also included for comparison with CDD_{DBT}. To transform the hourly weather data into monthly data, monthly climatic variables, including the monthly CDD_{DBT} and wet-bulb temperatures (CDD_{WBT}), monthly cooling hours, mean dry-bulb temperatures, mean wet-bulb temperatures, mean global solar radiation, and mean enthalpy, are calculated in this study. The monthly CDD_{DBT} and CDD_{WBT} are calculated as:

$$CDD_{DBT} = \sum_{i=1}^n (T_i - T_{bd})_{(for\ T_{bd} > T_i, (T_i - T_{bd}) = 0)} \quad (1)$$

$$CDD_{WBT} = \sum_{i=1}^n (T_i - T_{bw})_{(for\ T_{bw} > T_i, (T_i - T_{bw}) = 0)} \quad (2)$$

where T_i is the actual dry-bulb or wet-bulb temperature at the i th hour. T_{bd} is the base dry-bulb temperature, which is defined as 26 °C and is based on data from the Ministry of Housing and Urban-Rural Development in China (2005) ([Lee, Kok, Chan, Kong, & June, 2010](#)). T_{bw} is the base wet-bulb temperature, defined as 24 °C, and this temperature is the temperature at which the monthly CDD_{WBT} can provide the highest correlation coefficients with historical residential electricity consumption.

To represent different future pathways of GHG emissions and atmospheric concentrations, four trajectories of total radiative forcing are developed and represented by four representative concentration pathways (RCPs), namely, RCP2.6, RCP4.5, RCP6.0, and RCP8.5, which are contained in the Fifth Assessment Report (AR5) of the Intergovernmental Panel for Climate Change (IPCC). Different RCPs characterize different trajectories of total radiative forcing in 2100 compared with those of 1750 ([Knutti & Jan, 2013](#)). RCPs 4.5 and 8.5 represent intermediate stabilization and high greenhouse gas emissions, respectively, and are, believed to reflect the contrast between currently feasible and business-as-usual climate change mitigation goals ([Mora et al., 2013](#)). In contrast, RCP2.6 represents very low greenhouse gas emissions and is in agreement with ambitious climate change mitigation goals, and RCP6.0 portrays a high stabilization characteristic ([Mora et al., 2013](#)). However, only the RCP4.5 and RCP8.5 scenarios belong to the core experiments of the CMIP5 database and are provided by all GCM modeling groups ([Taylor, Stouffer, & Meehl, 2012](#)). The changing climate in Hong Kong is already on a track of medium and high emissions according to the last 5-year weather records from HKO ([Morakinyo et al., 2019](#)). Furthermore, the CO₂ emission trajectory under RCP8.5 exhibits the closest match to the current path of global CO₂ emissions ([Peters et al., 2013](#)), and the RCP4.5 scenario is regarded by researchers as the most likely scenario ([Zhu, Pan, Huang, & Xu, 2016](#)). Therefore, only RCP4.5 and RCP8.5 are chosen to represent future possible climate change scenarios. To obtain future local meteorological data, a statistical downscaling approach called the 'morphing' method is adopted in this study. The detailed process of this method is well documented in the literature by S. E. Belcher ([Belcher, Hacker, & Powell, 2005](#)) and in a previous Hong

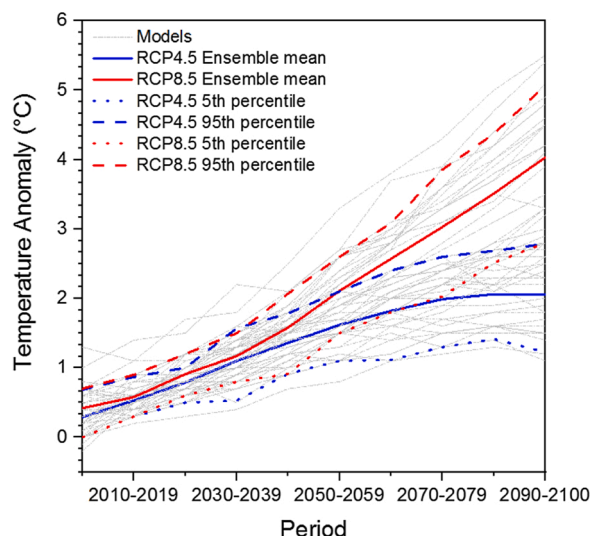


Fig. 3. Projected decadal temperature anomalies relative to 1979-2003 for Hong Kong under the RCP4.5 and RCP8.5 scenarios. Gray line represents output from a single GCM model; the red and blue solid curves represent the ensemble mean of the output under RCP4.5 and RCP8.5 scenarios; the 5th percentile and 95th percentile values are illustrated in dash lines. (For interpretation of the references to colour in this figure legend, the reader is referred to the web version of this article).

Kong case study (Liu, Kwok, Lau, Tong et al., 2020). Future weather datasets under different future RCP scenarios were extracted from 24 GCMs (<http://pcmdi9.llnl.gov>). These twenty-four models were selected because they provide finer spatial resolution, require climate variables, and both the RCP8.5 and RCP4.5 scenarios for projections. The historical outputs from 24 GCMs were already validated by HKO using cross-validation approaches (see Refs (Chan & Tong, 2014; Tong, Wong, & Lee, 2017)). All 24 GCMs are listed in Table A1 of the Appendix. Considering intermodel uncertainties, a prudent approach that uses the 5th percentile, 95th percentile and ensemble mean values from the outputs of multiple GCMs is adopted in this study (Troup, Eckelman, & Fannon, 2019). The projected 5th percentile, 95th percentile and ensemble mean values of decadal temperature anomalies from the different GCMs under different scenarios are shown in Fig. 3. The values of the projected 5th percentile, 95th percentile and ensemble mean of the temperature anomalies in each decade are also provided in Table A2 of the Appendix. Three time slices of the projected future weather data, 2026–2045 as the 2035s, 2056–2075 as the 2065s, and 2080–2099 as the 2090s, are classified to represent the near-term, middle-term, and long-term periods in this century. The future monthly climatic variables are also calculated based on Eqs. (1) and (2).

2.1.2. Socioeconomic variables

Long-term electricity consumption in a city can also be affected by

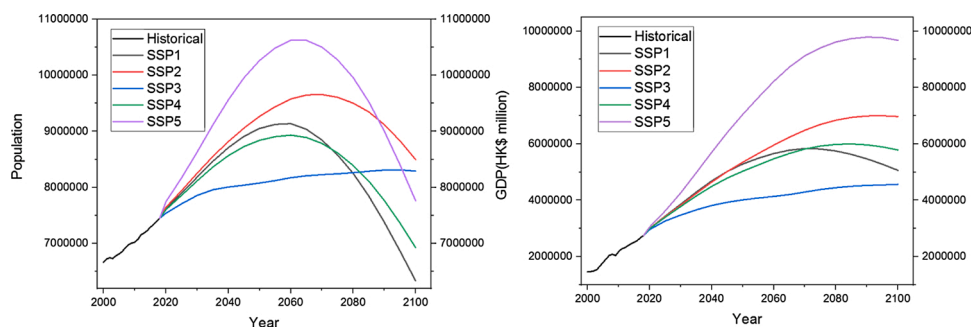


Fig. 4. Historical and projected data for GDP and population for Hong Kong under different shared social-economic pathway (SSP) scenarios.

multiple determinants, including technological, demographic and socio-economic variables. Several variables, such as population size, electricity prices, penetration rates of air conditioner use, GDPs (gross domestic product) and urbanization rates, have been commonly used in previous studies (e.g., Refs. (Santamouris (2016); Trotter, Bolkesjö, Férés, & Hollanda, 2016)). Although electricity price is one of the main factors which affects consumers in other nations or cities (Bianco, Manca, Nardini, & Minea, 2010; Fan et al., 2019), energy prices in Hong Kong are governed by the scheme of control (SOC) between the government and the two electricity suppliers. The historical data in Hong Kong show that electricity prices have had positive correlations, instead of generally inverse correlations, with electricity consumption levels since 1978 (Luk, 2005), which means that consumer demand has always exhibited an upward trend even if electricity prices have increased. Considering the availability and uncertainties of future electricity prices, energy prices are therefore not considered in the model. Additionally, as air conditioners have become a common domestic appliance in Hong Kong buildings, the penetration of air conditioners in Hong Kong has already reached more than 90 % in residential buildings and nearly 100 % in commercial buildings according to a survey conducted in 1998 (Wan & Yik, 2004), and technological innovation and new applications for replacing existing appliances have an ambiguous impact on electricity demand (Zheng et al., 2020); the further increase in penetration of air conditioners and technological changes are therefore ignored in our model.

However, long-term electricity demand is significantly affected, as has been widely recognized in the literature, by demographic and socio-economic factors. Population size and GDP are the most commonly used variables, as shown in Table 1. Moreover, future credible forecasts of these two variables are accessible for most nations in the world (Riahi et al., 2017). Therefore, set against the above considerations of dataset availability and local context, we chose to include population size and GDP in the model; we expect that these variables are more influential than some other variables on long-term electricity consumption. If the results of the model are well performed, there is little need to include additional variables. Historical GDP and population size data were obtained from the Census and Statistics Department of Hong Kong (2019b). Since the GDP data were recorded once per quarter, we perform a linear interpolation to obtain monthly GDP estimates. The quantitative projections of future GDP and population size are documented in the shared socioeconomic pathways (SSPs) database (<https://tntcat.iiasa.ac.at/SspDb>), and the narratives of socioeconomic development for the different SSPs are presented in Table A3 of the Appendix. The historical and projected data of GDP and population for Hong Kong in the 21 st century are presented in Fig. 4. The SSP framework is built around a matrix that combines RCPs and future socioeconomic SSP development pathways (O'Neill et al., 2014). To have time slices that are in concordance with the climate data of different RCPs, the socioeconomic data in the SSPs in the 21 st century are also divided into three periods: the 2035s, the 2065s, and the 2090s.

2.2. Data-driven methods

2.2.1. Support vector machine

SVMs are a popular supervised machine learning method for both classification and regression and are widely used in occupant behavior prediction, fault detection and diagnosis, image recognition and energy use prediction (Han, Kamber, & Pei, 2012). Following (Han et al., 2012) and applications as described in (Seyedzadeh, Pour Rahimian, Rastogi, & Glesk, 2019; Zhong et al., 2019), SVM can use a classifier to calculate the best hyperplane to separate the data points in an n-dimensional or infinite-dimensional space and divide them into two categories. SVM, when used as a regression method, which is called support vector regression (SVR), can also be transformed into SVR to predict energy use patterns. First, SVR uses a kernel function to sample data to a high-dimensional feature space. Then, the projection is performed through the linear regression equations as shown below:

$$f(x) = \sum_{i=1}^N (\alpha_i - \alpha_i^*) G(x_i, x) + \beta, \quad \beta \in R \quad (3)$$

$$s.t. \begin{cases} \sum_{i=1}^N (\alpha_i - \alpha_i^*) = 0 \\ 0 \leq \alpha_i, \alpha_i^* \leq C \end{cases} \quad (4)$$

where α_i and α_i^* are the Lagrange multipliers and C represents the penalty parameter. $G(x_i, x)$ is the kernel equation to project the original low-dimensional data to high-dimensional data.

Three popular kernel functions that are used in SVM applications are shown as follows:

Linear Kernel:

$$G(x_i, x) = x_i \cdot x \quad (5)$$

Radical Basis Function (RBF) Kernel:

$$G(x_i, x) = \exp(-\|x_i - x\|^2) \quad (6)$$

Polynomial Kernel:

$$G(x_i, x) = (1 + x_i \cdot x)^p \quad (7)$$

where p is a subset of the set $\{2, 3, \dots\}$.

By evaluating and comparing different kernels during the prediction training process, the most computationally efficient kernel can be identified as the linear kernel. The RBF kernel with the best accuracy is appropriate for dealing with nonlinear data.

2.2.2. Decision tree

DT is a supervised classification and regression method that utilizes a tree-structured flowchart to classify data points into their respective classes. Each internal node in the tree model, which is a nonleaf node, represents a test on an attribute (Yu, Haghghat, Fung, & Yoshino, 2010). Moreover, each leaf node determines whether a room air conditioner is on or off. To build a regression tree, there are two essential steps (James, Witten, Hastie, & Tibishirani, 2013):

“1. We divide the predictor space, which is the set of possible values for X_1, X_2, \dots, X_p —into J distinct and non-overlapping regions, R_1, R_2, \dots, R_J .

2. For every value that falls into the region R_j , same prediction will be made, which equals to the mean of the training observations’ response values in R_j .

The goal is to find boxes R_1, R_2, \dots, R_J , that minimize the RSS, given by

$$\sum_{j=1}^J \sum_{i \in R_j} (y_i - \hat{y}_{R_j})^2 \quad (8)$$

where \hat{y}_{R_j} is the mean response for the training observations within the J th box.”

2.2.3. Artificial neural network

ANNs are widely used machine learning algorithms that were inspired by biological neural networks (Kandananond, 2011; Ma & Cheng, 2016). The basic neural network model is usually based on a series of synaptic organizations of neurons, and the neural network can transform multiple inputs within the hidden layers. First, M linear combinations of the independent variables x_1, \dots, x_n are used, as shown in the following equation:

$$a_j = \sum_{i=1}^n w_{ji}^{(1)} x_i + w_{j0}^{(1)} \quad (9)$$

where the superscript (1) represents the parameters that belong to the first ‘layer’ and $j = 1, \dots, M$. The parameter $w_{ji}^{(1)}$ is the weight and $w_{j0}^{(1)}$ is the bias. Moreover, a_j are known as activation functions. Then, a differentiable, nonlinear activation function $h(\cdot)$ is provided to transfer each quantity as follows:

$$z_j = h(a_j) \quad (10)$$

The quantities that are in accordance with the outputs of the basis functions are called hidden units. A sigmoidal function such as the logistic sigmoid or ‘tanh’ function usually serves as a nonlinear activation function $h(\cdot)$. Again, these quantities are combined in linear form to generate output unit activation:

$$a_k = \sum_{j=1}^M w_{kj}^{(2)} z_j + w_{k0}^{(2)} \quad (11)$$

where $k = 1, \dots, K$ and K represent the total number of outputs. This transfer function reveals the second layer of the neural network and $w_{k0}^{(2)}$ is associated with the biases.

In summary, by using a suitable sigmoidal activation function, output unit activations can be transformed to calculate a set of outputs, y_k . For a standard regression problem, the activation function is the identity function to ensure that $y_k = a_k$. Finally, the above-described various stages can be integrated into one overall network function that can be represented as follows:

$$y_k(x, w) = \sigma \left(\sum_{j=1}^M w_{kj}^{(2)} h \left(\sum_{i=1}^D w_{ji}^{(1)} x_i + w_{j0}^{(1)} \right) + w_{k0}^{(2)} \right) \quad (12)$$

where vector w is the combination of all sets of weights and biases. Therefore, the framework of the network model can be interpreted as a nonlinear function that is based on input set $\{x_i\}$ with a corresponding output set $\{y_k\}$, and this function is also adjusted by the vector w .

2.2.4. Gradient boosting decision tree

GBDT models are ensemble methods that are based on DT (Touzani, Granderson, & Fernandes, 2018). Assuming we have K decision trees,

$$\hat{y}_i = \sum_{k=1}^K f_k(x_i), f_k \in F \quad (13)$$

where F is the space of functions to accommodate entire sets of regression trees and $f_k(x_i)$ represents a single tree.

The objective of GBDT is

$$Obj = \sum_{i=1}^n l(y_i, \hat{y}_i) + \sum_{k=1}^K \Omega(f_k) \quad (14)$$

where $\sum_{i=1}^n l(y_i, \hat{y}_i)$ is the training loss, and $\sum_{k=1}^K \Omega(f_k)$ is the complexity of trees.

Typical GBDT model training includes an iterative process to reach the maximum iteration number or minimum loss requirements.

2.2.5. Gaussian process regression

By using a Gaussian distribution, GPR models are powerful

nonparametric kernel-based probabilistic models for regression problems. Compared with other kernel-based methods such as SVM, some superior behaviors can be observed for GPR, e.g., learning the kernel and regularization parameters, overall feature selection, and making fully probabilistic predictions. The sample data in a typical GPR for prediction follow a marginal likelihood as follows:

$$p(y|X) \sim N(0, K_N + \sigma_n^2 I) \quad (15)$$

where $n \times n$ matrix K_N is the covariance matrix and σ_n^2 is the noise term's variance. Moreover, I is the identity matrix.

The predictive distribution is

$$p(y_*|X_*, X, y) \sim N(\mu_*, \sigma_*^2) \quad (16)$$

$$\mu_* = K_{*N}(K_N + \sigma_n^2 I)^{-1} y \quad (17)$$

$$\sigma_*^2 = K_{**} - K_{*N}(K_N + \sigma_n^2 I)^{-1} K_{N*} \quad (18)$$

which contains some key variables in GPR, e.g., μ_* is the mean value of the Gaussian posterior distribution, σ_*^2 is the covariance matrix in the regression problem, K_{*N} is the covariance matrix among the independent variables in the training and test sets, and σ_n^2 is the variance of the assumed noise level. Moreover, X and X_* represent the training inputs and new test inputs, respectively.

2.2.6. Multiple linear regression

MLR is a method to improve linear models to fit nonlinear functions to data, which utilizes the rapid computational performance of linear regression and enhances linear models to fit complex data curves. By constructing polynomial features from original inputs and coefficients, a multiple linear regression can be created based on polynomials with different orders or forms. For example, a traditional linear model with one-dimensional input data is shown as follows:

$$Y = a_0 X + b \quad (19)$$

When a complex function is fitted to the data instead of a hyperplane, we can combine the features of different-order polynomials:

$$Y = a_0 X + a_1 X^2 + a_2 X^3 + \dots + a_d X^d \quad (20)$$

where a_0, a_1, a_2, a_d are the coefficients, which can be readily determined using least squares linear regressions, since they can be estimated as standard linear regression models with predictors X, X^2, X^3, X^d . With a very large degree d , a polynomial regression can fit a very nonlinear curve, and in real-world practice, d is usually less than or equal to 4 (James et al., 2013). A degree that is too high can cause the curve to be overflexible and exhibit very strange shapes. In our research, the degree is strictly restricted to ≤ 4 .

2.3. Model validation and error calculation

To compare the performances among different algorithms, different widely used statistical criteria are adopted, including R-square, average deviation, coefficient of variance root mean squared error (CV-RMSE), mean absolute percentage error (MAPE) and normalized mean bias error (NMBE). For energy modeling practice, the standard of the American Society of Heating Refrigerating and Air-Conditioning Engineer (ASHRAE) Guideline 14 (ASHRAE Guideline 14-2014, 2014) recommends the use of two criteria, RMSE and NMBE, to evaluate the goodness-of-fit of a simulation model. Therefore, RMSE and NMBE were adopted to quantify the deviations among predicted values and actual values (Gayawan & Ipinoyomi, 2009). Instead of using classic RMSE, CV-RMSE was used as the statistical criterion to avoid ambiguity and achieve a more accurate evaluation. Results with lower CV-RMSE and NMBE values are normally preferred:

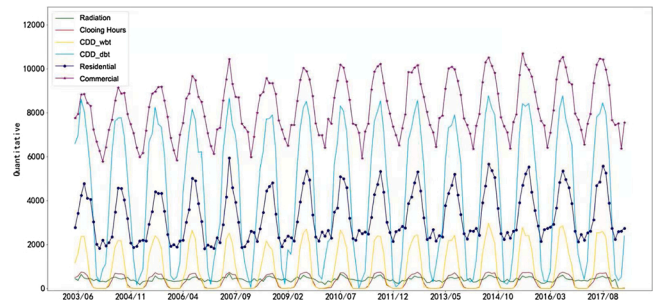


Fig. 5. Visualization of some principal meteorological variables and electricity consumption from 2003 to 2018.

$$NMBE(\%) = \frac{\sum_{i=1}^n (y_i - y'_i)}{n} \times \frac{1}{\bar{y}} \quad (21)$$

$$CV(RMSE)(\%) = \sqrt{\frac{\sum_{i=1}^n (y_i - y'_i)^2}{n}} \times \frac{1}{\bar{y}} \quad (22)$$

where y_i is the actual value, y'_i is the projected value at time interval i , and \bar{y} is the mean value of the total number of n real data points.

Another widely used statistical criterion, the average deviation, can quantify the averaged percentage deviation between the predicted and actual values of the entire dataset:

$$Average \ Deviation = \frac{\sum_{i=1}^n |y'_i - \bar{y}|}{n} \times 100\% \quad (23)$$

The mean absolute percentage error (MAPE) is another measurement of model perfection. This research used MAPE for comparisons of model accuracy, and smaller MAPE values indicate better performing models:

$$MAPE = \frac{1}{N} \sum_{i=1}^N \left| \frac{y_i - y'_i}{y_i} \right| \quad (24)$$

To avoid the negative effects of large sample sizes and extra explanatory variables, another coefficient of determination, adjusted R-square, was used to optimize R-square and to determine how well a model predicts new observations (Carpenter, Woodbury, & O'Neill, 2018). Predictions with higher adjusted R-square values are usually favored. The adjusted R-square measure is defined as follows:

$$Adjusted \ R - square = R^2 - (1 - R^2) \frac{p}{n - p - 1} = 1 - (1 - R^2) \frac{n - 1}{n - p - 1} \quad (25)$$

where n represents sample size, p is the total number of exploratory variables in the model, and R^2 is the abbreviation for R-square.

In this study, instead of using individual criteria, CV-RMSE and NMBE were used as the primary criteria, while the others were used as supplementary criteria. In addition, the annual deviations in time series and histograms of prediction deviations in the training and testing sets were plotted to determine the overall performances of different data-driven methods in terms of time series stability and generalization ability.

3. Results

3.1. Correlation results of independent variables and electricity consumption

Fig. 5 shows time series plots of key meteorological variables and electricity consumption from 2003 to 2018. Both residential and commercial electricity consumption exhibit clear seasonality, i.e., electricity

Table 2
Correlation matrix of electricity consumption against key independent variables from 1979 to 2018.

		Commercial	Residential	Enthalpy	CDD _{DBT}	CDD _{WBT}	Mean _{DBT}	Mean _{WBT}	Cooling Hours	Radiation	Population	GDP
Commercial	Pearson correlation value	1										
Residential	Pearson correlation value	.927**	1									
Enthalpy	Pearson correlation value	.269**	.457**	1								
CDD _{DBT}	Pearson correlation value	.279**	.475**	.990**	1							
CDD _{WBT}	Pearson correlation value	.248**	.493**	.869**	.899**	1						
Mean _{DBT}	Pearson correlation value	.276**	.460**	.996**	.987**	.854**	1					
Mean _{WBT}	Pearson correlation value	.266**	.447**	.991**	.978**	.864**	.985**	1				
Cooling Hours	Pearson correlation value	.254**	.489**	.926**	.956**	.966**	.917**	.914**	1			
Radiation	Pearson correlation value	.318**	.499**	.768**	.789**	.718**	.776**	.720**	.766**	1		
Population	Pearson correlation value	.943**	.811**	.067	.061	.050	.075	.070	.049	.104*	1	
GDP	Pearson correlation value	.944**	.822**	.097*	.094*	.085*	.104*	.097*	.081*	.157**	.953**	1

* Correlation is significant at the 0.05 level (2-tailed).

** Correlation is significant at the 0.01 level (2-tailed).

consumption in the summer months is significantly higher than that in the winter months. Peak electricity demand often occurs in July or August, while the minimum electricity demand often occurs during the winter months, such as December, January or February. In addition, electricity consumption generally tends to exhibit a similar trend to CDDs, which means that future electricity consumption will inevitably be high due to the increasing CDDs.

In this study, Pearson correlation coefficients were used to identify the relationships among different parameters. Table 2 shows the matrix of the Pearson correlation coefficients among electricity consumption in the residential and commercial building sectors and the influencing variables. Electricity consumption in the residential and commercial sectors is strongly influenced by meteorological parameters and socioeconomic variables, such as GDP, population, and CDD_{DBT}, with correlation coefficients of 0.822, 0.811, and 0.475 and 0.944, 0.943, and 0.279 for the residential and commercial sectors, respectively. Over the 40-year period, socioeconomic variables tended to have more influence on electricity consumption than meteorological variables, which indicates that future long-term socioeconomic development could provide the dominant influence on future electricity demand. The results also suggest that socioeconomic development is more closely related to the

increased electricity consumption in the commercial sector, i.e., the correlation coefficients among the socioeconomic variables and electricity consumption in the commercial sector are larger than those in the residential sector. On the other hand, electricity consumption in the residential sector is more sensitive to climatic variables, e.g., CDDs and radiation. In addition, the results suggest that several independent variables, such as CDDs, enthalpy, mean dry-bulb and wet-bulb temperatures and cooling hours, have significant intercorrelations and collinearity among them. However, CDD_{DBT} has a higher correlation coefficient than CDD_{WBT}, cooling hours, enthalpy, and mean dry-bulb and wet-bulb temperature for the commercial sector, while CDD_{WBT} is more strongly related to the residential sector than the other meteorological variables. This finding means that CDDs based on dry-bulb or wet-bulb temperatures are still more influential than the other meteorological variables for electricity consumption in Hong Kong. Therefore, only those variables with higher correlation coefficients, e.g., CDD_{DBT}, CDD_{WBT} and solar radiation, are included as independent meteorological variables for model training.

Table 3
Comparison of statistical criteria and computation times for the residential sector.

Algorithm	Deviation Percentage (%)	R2	CV-RMSE	NMBE	MAPE	Computation time
SVR	-7.6736	0.8878	369.9767	8.5264	8.1303	0.1448
Decision Tree	-7.1397	0.8468	432.3404	9.8444	6.7301	0.0548
ANN	13.9773	0.6189	681.8645	17.7908	-13.0189	1.0027
GBDT	-7.4762	0.8839	376.4297	9.1091	7.9868	0.0801
GPR	-0.6037	0.8418	439.4031	10.1600	9.9375	1.9865
MLR	5.3376	0.8689	399.9245	9.5315	-6.4693	0.1848

Table 4
Comparison of statistical criteria and computation times for the commercial sector.

Algorithm	Deviation Percentage (%)	R2	CV-RMSE	NMBE	MAPE	Computation time
SVR	2.2248	0.9070	392.9819	3.7017	-1.9996	0.0480
Decision Tree	-5.1804	0.7946	584.0735	5.5243	5.4079	0.0250
ANN	14.4964	0.2937	1465.6920	14.6236	-14.2842	3.9562
GBDT	-3.4467	0.8957	416.0928	4.0818	3.7180	0.1326
GPR	-1.2049	0.7986	578.3119	4.9640	3.5756	2.4120
MLR	4.7388	0.7691	619.1794	6.0161	-4.6745	0.3152

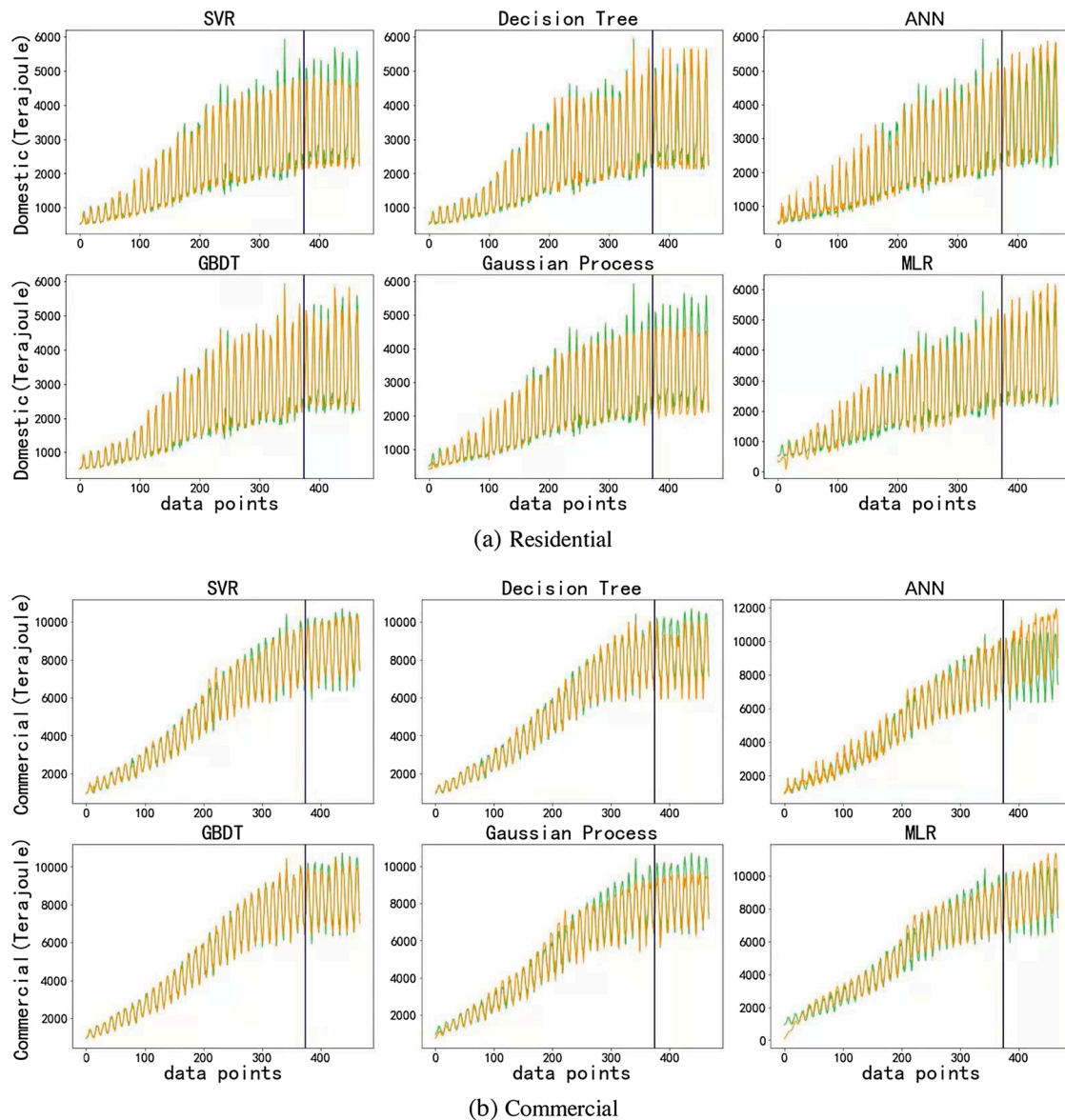


Fig. 6. Visualizations of training data and test data and their prediction results for (a) the residential sector and (b) commercial sector. Orange lines represent simulated values, while the green lines represent actual values. Blue vertical lines reveal the separation boundaries between the training and testing data, where the left part of the figure is the training set, and the testing set is shown in the right part. (For interpretation of the references to colour in this figure legend, the reader is referred to the web version of this article).

3.2. Comparisons of model performance

Six statistical criteria, which included deviation percentage, R-square, CV-RMSE, MAPE and NMBE, are used to evaluate prediction accuracies, as shown in Table 3 for the residential sector and Table 4 for the commercial sector. Normally, the preferred algorithms for energy predictions demonstrate the shortest computation time, NMBE,

deviation percentage and CV-RMSE and with the highest R-square value. The results show that the deviation percentage, adjusted R-square, CV-RMSE, NMBE, and MAPE values vary for different methods, but no single method performed best among the different criteria. For computing times, all algorithms exhibit a quick response and their computation times are all less than 4 s, while the GPR and ANN usually involve longer times, i.e., more than 1 s, to generate predictions, which

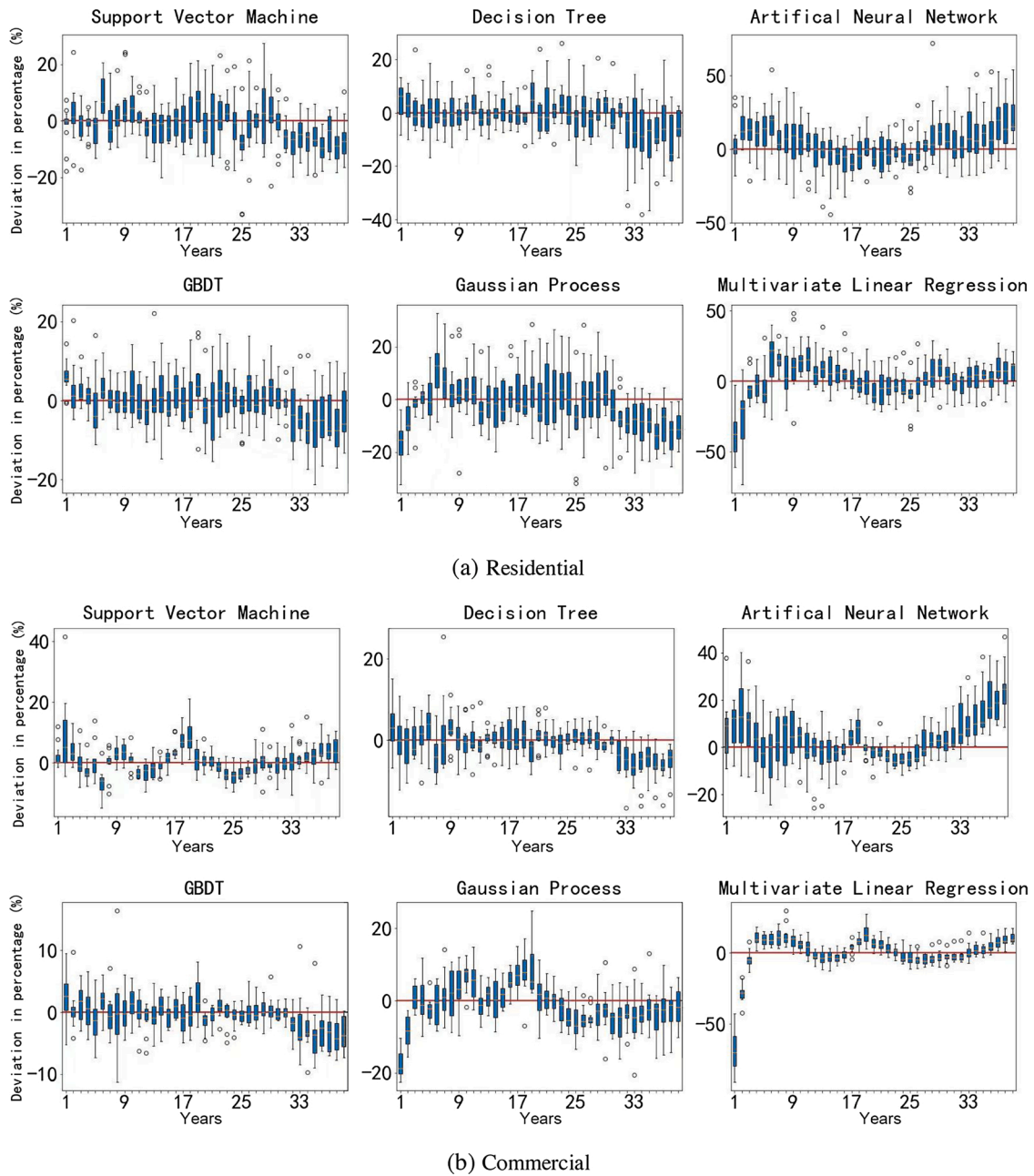


Fig. 7. Visualizations of the annual predictions of the relative deviations shown as box plots in (a) the residential sector and (b) the commercial sector. Note that the axis ranges are different among some methods.

means that the algorithm architecture in the GPR and ANN methods is more complex than in the others. In the residential sector, the R-square, RMSE, and NMBE values of the ANN model are 0.6189, 681.8645 and 17.7908, respectively. Among all algorithms, the ANN model demonstrated the lowest prediction accuracy. For the remaining algorithms, the DT and GPR models exhibit higher CV-RMSE and NMBE values than the other methods, while the SVR, GBDT and MLR methods have similar performances with higher precisions. For the commercial sector, although there is no significant difference among the different algorithms in terms of CV-RMSE and NMBE, the exception is that the ANN model exhibits relatively lower accuracy, i.e., all statistical criteria in the ANN method are inferior to the other algorithms. In contrast, the CV-RMSE values of the SVR and GBDT algorithms are 392.9819 and 416.0928, respectively, which are smaller than those of the other models and indicate that the SVR and GBDT algorithms have the best ability to predict overall load shapes. In summary, the SVR, GBDT and MLR

algorithms exhibit better prediction performances for the residential sector. The SVR and GBDT algorithms exhibit better performance for the commercial sector in terms of their accuracies.

However, based on the abovementioned statistical criteria, determining the best-performing algorithm is not straightforward. Since using single statistical criteria to describe entire datasets and predict results is flawed, i.e., the criteria can hardly express the information for an entire time-series, time series plots for all prediction methods are presented in this study, as shown in Fig. 6. For the residential sector, Fig. 6(a) reveals that although the SVR and GPR algorithms exhibit very strong overall performance for the training data, they tend to have overfitting issues for the testing data. In particular, these algorithms exhibit poor performances for predicting the peak electricity consumption of each year in the testing data. This result means that they have weaker generalization abilities than the other methods. For the remaining methods, the ANN model exhibits weak performance for the

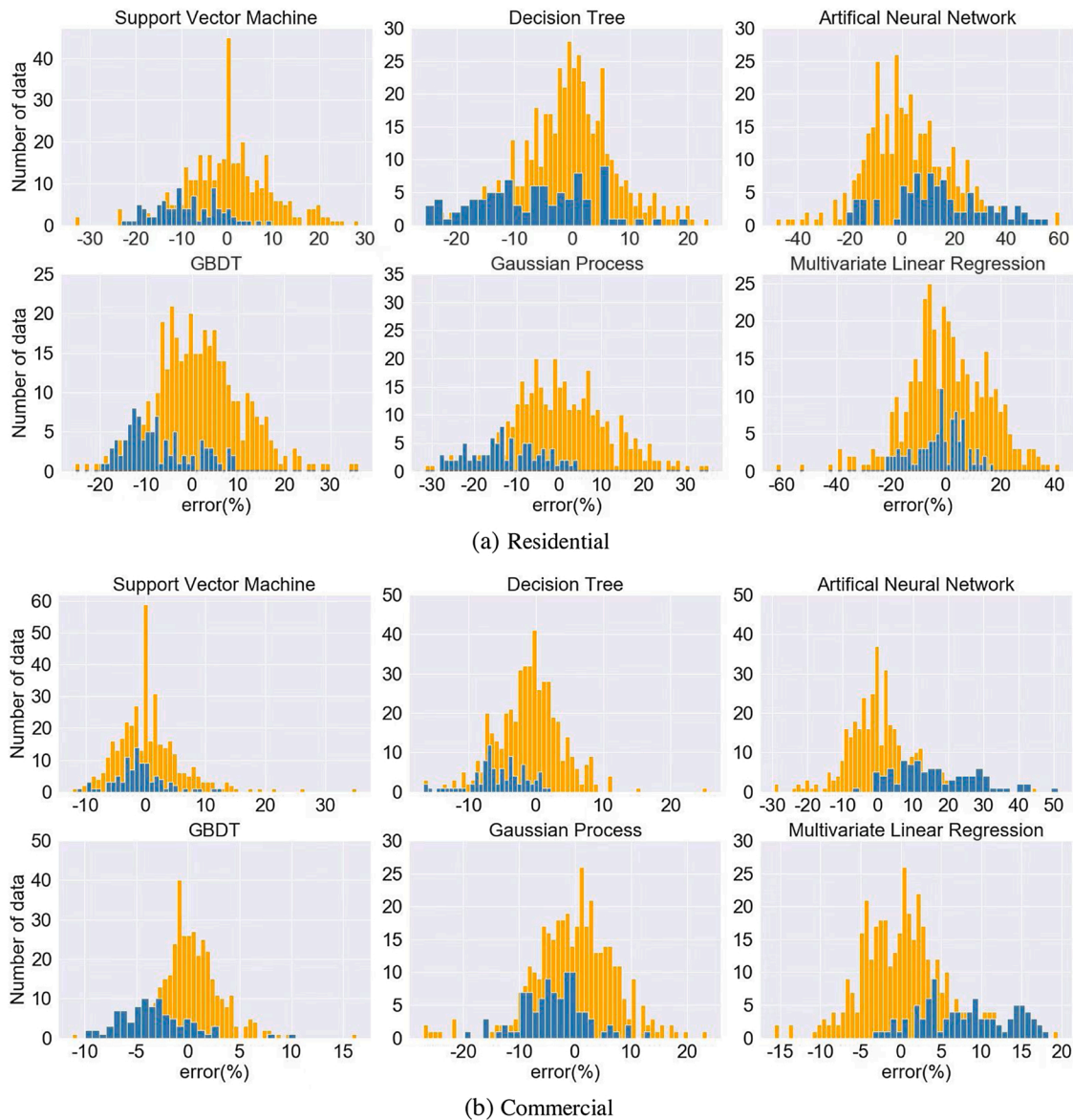


Fig. 8. Histogram visualizations of the predicted relative deviations of (a) the residential sector and (b) commercial sector. Orange colors indicate the deviations for the training set, while the blue colors indicate the deviations for the testing set. Note that the axis ranges are different among some methods. (For interpretation of the references to colour in this figure legend, the reader is referred to the web version of this article).

lowest electricity usage levels in the last years of the testing set, while the decision tree, GBDT and MLR algorithms exhibit better performance for the testing set than the other methods. However, among the decision tree, GBDT and MLR methods, their results appear to present similar behavior and small differences in terms of their generalization ability. Thus, additional exploration is needed to identify the best algorithm.

Time-series plots for the commercial sector are shown in Fig. 6(b). These show that although most of the algorithms exhibit good performance for the training data, the DT, ANN, GPR and MLR methods tend to show overfitting for the testing data, which indicates their weaker generalization abilities for long-term commercial electricity demand predictions compared with other methods. Specifically, the GPR and DT models cannot reasonably predict the peak electricity consumption of each year in the testing data, while the ANN and MLR models perform poorly for determining the lowest energy use levels in the recent few years. Only the GBDT algorithm shows a smaller discrepancy with actual electricity consumption and appears to be satisfied, which reveals the superiority and greater generalization ability of the GBDT algorithm for the commercial sector when compared with other methods. Therefore,

the GBDT algorithm is identified as the best-performing algorithm for commercial energy use predictions in terms of generalization ability.

Fig. 7 shows the annual relative deviations between the predicted results for the different algorithms and the actual values from 1979 to 2018. For the residential sector, smaller annual relative deviations are evident for the DT and GBDT models, which mean that using tree-based models in energy use predictions provides greater accuracy with time. Furthermore, Fig. 8 shows comparisons of the actual and predicted values by using histograms, in which thinner symmetrical shapes are favored. Similar characteristics for the GBDT performance can be found in both the residential and commercial sectors, i.e., the performance of the results using the GBDT method exhibits better stability and accuracy with more symmetrical shapes and fewer significant deviations than the other algorithms. However, due to the size of the dataset, the deviation histogram does not represent an ideal Gaussian distribution. It should be noted that different algorithms tend to reduce the absolute deviations of the predictions, but large relative deviations can still be observed in the initial years of the dataset due to the lower total electricity use.

Additionally, comparing the training data with the testing data

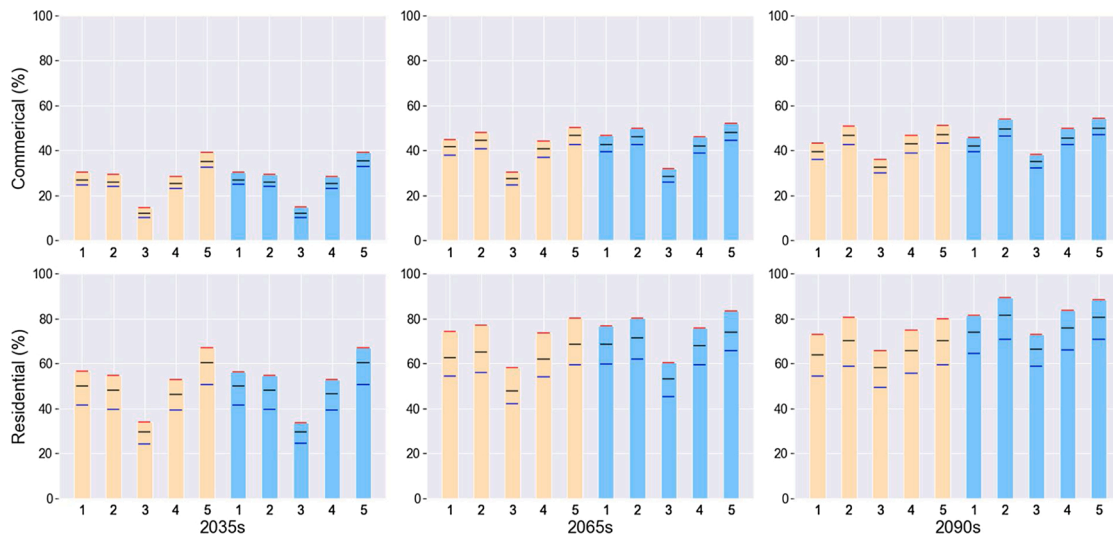


Fig. 9. Percentage changes of future electricity prediction under different climate change and socioeconomic scenarios compared with electricity consumption in 2018. Different numbers indicate different SSP scenarios. The different-colored lines in red, black and blue indicate the 95 % percentile, ensemble mean and 5% percentile, respectively. Orange and blue bars indicate RCP4.5 and RCP8.5, respectively. (For interpretation of the references to colour in this figure legend, the reader is referred to the web version of this article).

(Fig. 8) indicates that there are no significantly different deviation ranges and patterns in the GBDT data for the residential sector and in the SVR and GBDT data for the commercial sector, while weaker generalization abilities and significant overfitting issues can be observed for the other methods. Overall, the performance results of the GBDT method show that it not only has a greater generalization ability and higher prediction accuracy but also provides better stability in time series than the other algorithms. Therefore, we infer that the GBDT method provides more accurate and reliable predictions than the five other methods for the long-term electricity consumption for both the residential and commercial sectors.

3.3. Predictions of future electricity demand under different climate change and socioeconomic scenarios

Fig. 9 shows the percentage changes of future electricity demand in the residential and commercial sectors under different climate change and socioeconomic scenarios. It can clearly be seen that electricity demand is expected to increase in all scenarios over time and that the relative increase in electricity demand in the residential sector is considerably larger than that in the commercial sector. The increasing trend of electricity demand is expected to be more dramatic before

2065s and then less pronounced from 2065s to 2090s. Moreover, the discrepancy between different percentiles increases with time. For instance, the difference between the 5th and 95th percentiles in the residential sector under SSP3 and the RCP8.5–2030 s scenario is 9.3 %, but the difference between them in SSP3 becomes 14.3 % under the RCP8.5–2090 s scenario. These results also confirm that the implications of the different percentiles of GCMs on electricity demand could be larger than the implications of different RCPs, e.g., the difference between RCP4.5 and RCP8.5 in SSP1–2035s is only 0.19 %, while the difference between the 5th and 95th percentiles in RCP4.5 and SSP1–2035s is 9.75 %. Which illustrates that the divergence among different GCMs must be considered instead of being eliminated. This result agrees with the temperature differences among different GCMs, as shown in Fig. 3, and IPCC AR5, which states that the variations across the different GCMs could be larger than those among different RCPs.

In contrast, SSPs have significantly varied impacts on electricity demand under a given RCP. Among the different SSPs, the lowest electricity demand is always found for SSP3, while the highest demand is found for SSP5 in 2035s and 2065s and for SSP2 in 2090s. These findings can be obtained due to the different increase rates of SSPs, as shown in Fig. 3. For example, the smallest GDP and population can be found in SSP3 from 2035s to 2065s, while the population decrease that takes

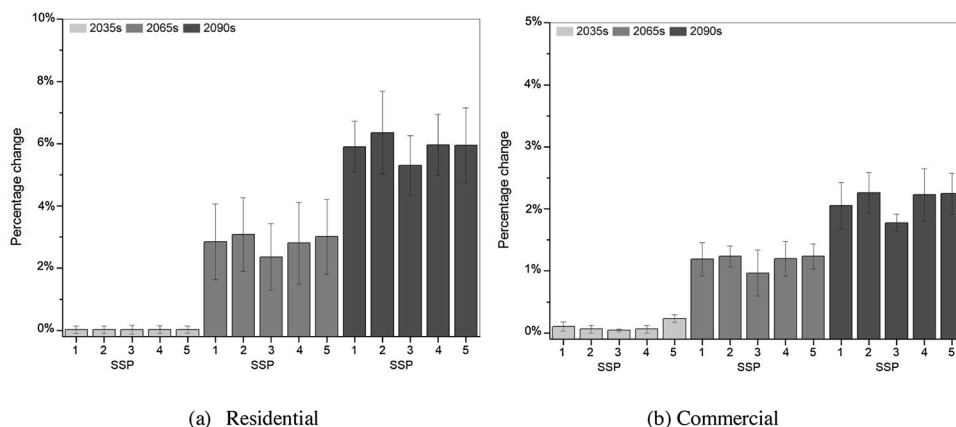


Fig. 10. Relative percentage changes between RCP8.5 and RCP4.5 under the different SSPs. The error bars indicate the standard deviations between the different percentiles.

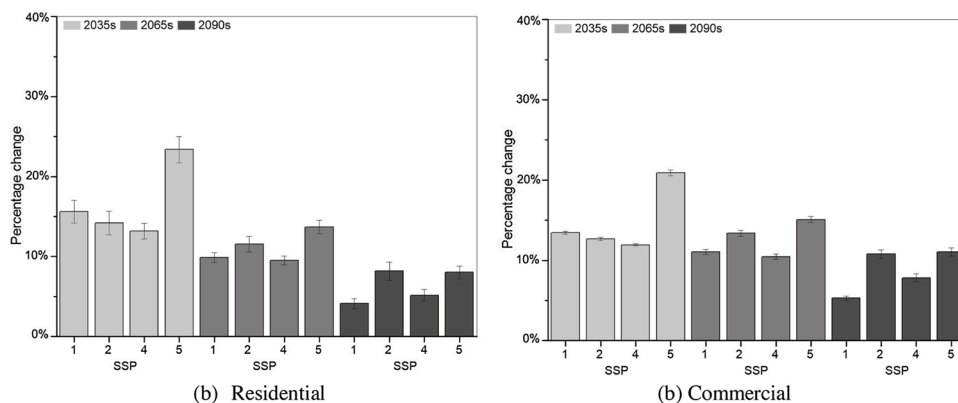


Fig. 11. Relative percentage changes among the different SSPs and SSP3. The error bars indicate the standard deviations among the different percentiles and RCPs.

place for SPP5 is more dramatic than for the other SPPs from the 2065s to 2090s and the population in SSP2 is the largest in 2090s. Another characteristic is that the divergence of electricity demand among different SSPs decreases with time. For example, the difference between electricity demand in SSP3 and SSP5 can be up to 26.5% in 2035s for the residential sector, but the maximum differences between SSP3 and SSP5 become 10.2% in 2065s and 2090s, respectively. The reason is that the GDP and population of SSP3 are the lowest among SSPs before the 2065s but steadily increase after that time, while they decrease in the other SSPs after the 2065s.

To compare the magnitudes of the implications among the different climatic scenarios and socioeconomic development scenarios, the relative percentage changes among the different RCP and SSP scenarios are presented in Figs. 10 and 11. Fig. 10 shows the percentage changes of electricity demand between RCP8.5 and RCP4.5 by using the electricity demand in RCP4.5 as the baseline. The results show that variations in RCP scenarios can cause greater increases in electricity demand in the residential sector (from a 5%–7% increase in the 2090s) than in the commercial sector (from a 1.5%–2.5% increase in the 2090s). This effect could be attributable to the higher sensitivity, i.e., higher correlation coefficients, of the residential electricity demand to climate change than the commercial sector, as stated in Section 4.1. RCP8.5, with higher radiative forcing, means higher CDDs than RCP4.5, and the differences in CDDs will become larger with time, as shown in Fig. 3. Thus, the variations in RCP scenarios lead to higher electricity demand in the 2090s than in the 2035s and 2065s.

Fig. 11 shows the percentage changes among different SSPs when using the smallest SSP3 as the baseline. Overall, the ratios of variations among SSPs are higher than those among RCPs. The variations among different SSPs could result in a 10%–25% change in electricity demand in the 2035s and a 5%–12% change in the 2090s. However, the results reveal that the divergence of electricity demand among different SSPs decreases with time. Although the increase in electricity demand that is caused by climate change becomes more significant over time, the influence of the variations in SSPs on the increase in electricity demand decreases in the 2090s. This finding could also explain why the overall increasing trend of electricity demand is more dramatic before 2065 and becomes lower from 2065 to 2090. Notably, the percentage change that is attributable to socioeconomic development in the residential sector is larger than that in the commercial sector in the 2035s, while the change in long-term electricity demand in the commercial sector that is caused by socioeconomic development is larger than that in the residential sector in the 2090s. The reason could be that electricity demand in the commercial sector is more sensitive to long-term socioeconomic variables than the residential sector. Moreover, larger deviations that are attributable to climate change can be found in the residential sector, which further confirms the higher sensitivity of residential electricity demand to climate change and helps explain the greater increase in

electricity demand in residential buildings than in commercial buildings.

4. Discussion

4.1. Performance of data-driven methods

After cross comparing the performances among the six popular data-driven methods, the ANN method provides results with the lowest accuracy, while the GBDT method outperforms the other methods. In fact, most previous studies (Kandananond, 2011; Kankal et al., 2011; Sangrody et al., 2018) have stated that the ANN is better than the MLR and other linear regression methods. Although direct comparisons are not possible, as none of these comparisons simultaneously considered the GBDT, MLR and ANN methods, the reason behind the different performances of the ANN and MLR could be attributed to the differences in training datasets and independent variables between this study and previous studies. For instance, previous studies (Kandananond, 2011; Kankal et al., 2011; Sangrody et al., 2018) only considered climatic variables or socioeconomic variables over shorter historical periods (typically from 15 to 20 years) as input data, but our model considered 40-year climatic and socioeconomic variables together. Therefore, the long-term synergistic effect of socioeconomic development and climate change could perform differently. Although most of the data-driven models have demonstrated their ability to use small numbers of independent variables to infer energy use with long computation times, small error qualification, and efficiency in hyperparameter tuning, the GBDT method is finally selected to develop long-term monthly electricity demand modeling due to its higher accuracy, better generalization ability, and time series stability. Notably, the performance of these data-driven models is influenced considerably by the long-term characteristics of the particular dataset used in this study. Hong Kong underwent significant economic and population growth during the second half of the 20th century and showed signs of slowing down at the beginning of this century. This long-term socioeconomic property could affect overall model performances because the prediction model is significantly affected by socioeconomic variables as well as by the duration of the training data. Moreover, city-scale datasets are usually of small size with limited known predictors, which could also affect the performance of data-driven models.

4.2. Climatic and socioeconomic impacts and policy implications

The uncertainties that arise from future climate change and socioeconomic scenarios are all considered in the model. The results show that socioeconomic variables are strongly related to historical electricity consumption and are the main drivers of the increased electricity demand. This conclusion is affirmed by previous case studies (Fan et al.,

2019; Lam, 1998; Pili-Sihvola, Aatola, Ollikainen, & Tuomenvirta, 2010). In addition, the increasing trend of future electricity consumption that is projected by our model, which peaks in the 2065s due to the greatest increase in GDP and population at that time, is verified by other studies in the same regions (Fan et al., 2019; Zheng et al., 2020). However, some studies have used regression models in other regions, e.g., Brazil (Trotter et al., 2016) and Iran (Toktarova, Gruber, Hlusiak, Bogdanov, & Breyer, 2019) and have predicted that peak electricity consumption will occur from 2060 to 2080. In contrast, our model predicts that electricity consumption is still expected to increase slightly after 2065s. This result could be attributable to the differences in climatic and socioeconomic development contexts and modeling methods. Moreover, the residential and commercial sectors exhibit different responses to climate change. The residential sector of this study is 2–3 times more sensitive to RCP changes than the commercial sector. Similar results can be found in previous studies (Fung, Lam, Hung, Pang, & Lee, 2006; Lam, Wan, Lam, & Wong, 2010) of Hong Kong. However, the percentage changes of electricity demand are different compared with previous studies. For instance, Wan, Li, Liu, & Lam, 2011 explored the increasing trend of cooling loads caused by climate change in Hong Kong by using regression models. They reported that electricity consumption would increase by 6.3% and 7.6% in 2070–2100 for the low-forcing and medium-forcing climate change scenarios, respectively. Two other studies (Kolokotsa & Santamouris, 2015; Wan, Li, & Lam, 2011) also estimated that the percentage increases in energy use in 2090–2100 are expected to increase by up to 8.1% and 10.7% compared with the average energy use in 1979–2008 using regression analysis, respectively. In contrast, the total electricity demand for buildings may increase by up to 89.40% in the residential sector and by 54.34% in the commercial sector compared with the 2018 levels presented in this study. The reason for this difference is mainly due to the lack of consideration of socioeconomic development variables in the previous models and the different climate change scenarios and GCMs adopted, i.e., a special report on emissions scenarios (SRES) and Coupled Model Intercomparison Project Phase 3 (CMIP3), in the previous studies.

The results also show that although there are no significant differences in future total energy demand under different RCPs in the near-term 2035s, while a large increasing trend for the residential sector is still observed. These findings also suggest that climate change mitigation policy interventions, such as adopting clean and renewable energy technologies and green building designs, should be implemented. Otherwise, a significant electricity demand increase will be inevitable and will further intensify GHG emissions and global climate change. The inevitably increasing electricity demand requires significant additional investments to enhance power capacity, which may also lead to increased costs of energy management and electricity prices and exacerbate the vulnerability of the low-income population (Kolokotsa & Santamouris, 2015). Therefore, climate change policy interventions, such as mitigation of climate change and energy efficiency retrofitting measures for existing buildings, should be implemented urgently to achieve 2025 energy saving and 2030 carbon emission reduction targets, as stated in Hong Kong Energy Saving Planning 2025+ (Development Bureau & Transport & Housing Bureau, 2015) and Hong Kong Climate Action Plan 2030+ (Environment Bureau, 2017). Policies that aim to place stringent limits on resource usage and enhance the sinks of temperature anomalies, such as the use of renewable energy technologies, high energy efficiency supply and management systems, and smart and resilient technologies for cities, in association with mitigation technologies for urban infrastructure and buildings, could significantly reduce GHG emissions and future energy demands (Santamouris, 2013). The Buildings Department in Hong Kong controls the energy efficiency of residential and commercial buildings by setting thresholds for the residential thermal transfer value (RTTV) and overall thermal transfer value (OTTV), respectively. This study also provides evidence of the pressing need to review both the OTTV and RTTV standards and to continue enhancing these two standards over time in the context of

future climate change. In addition to using technological measures, energy-conserving behaviors among the general public and households should also be encouraged and considered as a key adaptation policy option (Yang, Yan, & Lam, 2014).

4.3. Limitations and future work

Since this study explicitly focuses on the impacts of long-term future climate change and socioeconomic development on monthly electricity demands, day-to-day or hourly predictions are limited due to the unavailability of higher-resolution historical electricity consumption data. However, the climatic data, methods and framework of this study would also be applicable for more useful daily or hourly electricity demand forecasts if daily or hourly historical electricity consumption data were available in the future. Additionally, the GBDT algorithm should be updated with additional parameters to improve prediction accuracies in the future. In addition to these temporal limitations, this study uses only the aggregated datasets at the city scale. Hence, the spatial-temporal variations in electricity consumption and effective return periods of renewable energy plans could be further studied.

5. Conclusion

Long-term predictions of electricity demand while considering both future climate change and socioeconomic growth are of great interest for policymakers to manage energy systems, control carbon emissions and develop climate change mitigation strategies at the city level. This study focuses on (1) testing and applying six popular data-driven methods, including SVM, DT, ANN, GBDT, GPR and MLR, for long-term electricity predictions at the city scale; (2) analyzing and cross-comparing their simulation performances in terms of accuracy, stability, and generalization ability to identify the best model; and (3) adopting the GBDT model, which is the most suitable model, in a case study in Hong Kong to predict long-term monthly electricity demands under both future climatic and socioeconomic changes.

The following major contributions and conclusions can be drawn:

- 1 The prediction accuracies of six popular data-driven methods are compared by examining their computational times and statistical criteria, including deviation percentage, R-square, CV-RMSE, MAPE and NMBE. SVR, GBDT and MLR to achieve better prediction accuracy for the residential sector. The SVR and GBDT methods exhibit better performance for the commercial sector in terms of CV-RMSE and NMBE. Compared with the other commonly used data-driven models, the GBDT algorithm demonstrates its overall superiority with respect to its accuracy, generalization ability, and time series stability. Based on the findings detailed above, it is easy for other researchers to select an appropriate data-driven model based on their study purpose and needs.
- 2 The uncertainties that arise from both future climate change and socioeconomic scenarios are considered in the model. To examine the future uncertainties of different RCPs, GCMs and socioeconomic development, a matrix that combines the projected 5th percentile, 95th percentile and ensemble mean values of temperature anomalies from 24 GCMs under different RCP scenarios and socioeconomic data, i.e., GDP and population, of different socioeconomic SSP development pathways are adopted in the selected prediction model. This study not only provides a comprehensive method for combining both climate change and socioeconomic conditions into prediction simulations but also considers the potential uncertainties to achieve higher accuracy and reliability of simulation results.
- 3 Long-term predictions of electricity demand that are obtained by applying the GBDT model considering different future climatic change scenarios and socioeconomic uncertainties are demonstrated and recommended; these predictions can provide reliable and useful scientific-based evidence for developing energy saving plans,

managing urban carbon emissions, and mitigating climate change in the 21 st century. The case study in Hong Kong demonstrates that a future changing climate together with socioeconomic development can result in significant increases in monthly electricity demand. This demand is expected to increase by up to 89.40 % for the residential sector and by 54.34 % for the commercial sector in the 2090s compared with 2018 levels. Practically, the study provides an important reference for local policymakers but also provides a useful demonstration example for future energy predictions for other sub-tropical cities.

Declaration of Competing Interest

The authors declare that they have no known competing financial interests or personal relationships that could have appeared to influence the work reported in this paper.

Table A1

List of CMIP5 general circulation models applied in this study (Liu, Kwok, Lau, Tong et al., 2020).

Model Designation	Modelling Group	Group Acronym	Scenarios
ACCESS1-0	Commonwealth Scientific and Industrial Research Organization	CSIRO	RCP4.5, RCP8.5
BCC-CSM1-1	Beijing Climate Center, China Meteorological Administration	BCC	RCP4.5, RCP8.5, RCP2.6, RCP6.0
BNU-ESM	College of Global Change and Earth System Science, Beijing Normal University	GCESS,BNU	RCP4.5, RCP8.5, RCP2.6
CanESM2	Canadian Centre for Climate Modelling and Analysis	CCCma	RCP4.5, RCP8.5, RCP2.6
CNRM-CM5	Centre National de Recherches Météorologiques	CNRM	RCP4.5, RCP8.5, RCP2.6
CSIRO-Mk3-6-0	Commonwealth Scientific and Industrial Research Organization	CSIRO	RCP4.5, RCP8.5, RCP2.6, RCP6.0
GFDL-ESM2G	NOAA Geophysical Fluid Dynamics Laboratory	NOAA GFDL	RCP4.5, RCP8.5, RCP6.0
GFDL-ESM2M	NOAA Geophysical Fluid Dynamics Laboratory	NOAA GFDL	RCP4.5, RCP8.5, RCP6.0
HadGEM2-CC	Met Office Hadley Centre	MOHC	RCP4.5, RCP8.5
INM-CM4	Institute for Numerical Mathematics	INM	RCP4.5, RCP8.5
IPSL-CM5A-LR	Institut Pierre-Simon Laplace	IPSL	RCP4.5, RCP8.5, RCP2.6, RCP6.0
IPSL-CM5A-MR	Institut Pierre-Simon Laplace	IPSL	RCP4.5, RCP8.5, RCP2.6, RCP6.0
IPSL-CM5B-LR	Institut Pierre-Simon Laplace	IPSL	RCP4.5, RCP8.5
MIROC5	Japan Agency for Marine-Earth Science and Technology, Atmosphere and Ocean Research Institute, The University of Tokyo	MIROC	RCP4.5, RCP8.5, RCP2.6, RCP6.0
MIROC-ESM	Japan Agency for Marine-Earth Science and Technology, Atmosphere and Ocean Research Institute, The University of Tokyo	MIROC	RCP4.5, RCP8.5
MIROC-ESM-CHEM	Japan Agency for Marine-Earth Science and Technology, Atmosphere and Ocean Research Institute, The University of Tokyo	MIROC	RCP4.5, RCP8.5, RCP2.6, RCP6.0
MPI-ESM-LR	Max-Planck-Institut für Meteorologie	MPI	RCP4.5, RCP8.5, RCP2.6
MRI-CGCM	Meteorological Research Institute	MRI	RCP4.5, RCP8.5, RCP6.0
Nor-ESM1-M	Norwegian Climate Centre	NCC	RCP4.5, RCP8.5, RCP2.6, RCP6.0
MPI-ESM-MR	Max-Planck-Institut für Meteorologie	MPI	RCP4.5, RCP8.5, RCP2.6
ACCESS1-3	Commonwealth Scientific and Industrial Research Organization	CSIRO	RCP4.5, RCP8.5
BCC-CSM1-1-m	Beijing Climate Center, China Meteorological Administration	BCC	RCP4.5, RCP8.5, RCP2.6, RCP6.0
CMCC-CMS	Centro Euro-Mediterraneo per I Cambiamenti Climatici	CMCC	RCP4.5, RCP8.5
CMCC-CM	Centro Euro-Mediterraneo per I Cambiamenti Climatici	CMCC	RCP4.5, RCP8.5

Table A2

The ensemble mean, 5th percentile, and 95th percentile of temperature anomaly in each decade under the different RCP scenarios.

Period	RCP4.5			RCP8.5		
	5th percentile	The ensemble mean	95th percentile	5th percentile	The ensemble mean	95th percentile
2000–2009	0	0.29	0.69	0	0.42	0.70
2010–2019	0.30	0.53	0.87	0.30	0.58	0.90
2020–2029	0.50	0.79	1.00	0.60	0.91	1.20
2030–2039	0.53	1.10	1.57	0.80	1.17	1.50
2040–2049	0.92	1.36	1.79	0.92	1.58	2.07
2050–2059	1.10	1.62	2.10	1.50	2.11	2.60
2060–2069	1.12	1.82	2.40	1.80	2.57	3.09
2070–2079	1.30	1.99	2.60	2.03	3.03	3.86
2080–2089	1.42	2.06	2.69	2.52	3.51	4.37
2090–2099	1.23	2.06	2.79	2.80	4.03	5.07

Table A3
Shared Socioeconomic Pathways (SSPs) narratives (O'Neill et al., 2014).

SSPs	Characteristic	Challenges
SSP1	Sustainability	Low challenges to mitigation or adaptation
SSP2	Middle of the road	Intermediate challenges
SSP3	Fragmentation	High challenges to both mitigation and adaptation
SSP4	Inequality	Low challenges to mitigation, but high adaptation challenges
SSP5	Conventional development	Low challenges to adaptation, but high mitigation challenges

References

- Ahmed, T., Muttaqi, K. M., & Agalgaonkar, A. P. (2012). Climate change impacts on electricity demand in the State of New South Wales, Australia. *Applied Energy*, 98, 376–383. <https://doi.org/10.1016/j.apenergy.2012.03.059>
- Andrić, I., Koc, M., & Al-Ghamdi, S. G. (2019). A review of climate change implications for built environment: Impacts, mitigation measures and associated challenges in developed and developing countries. *Journal of Cleaner Production*, 211, 83–102. <https://doi.org/10.1016/j.jclepro.2018.11.128>
- Ang, B. W., Wang, H., & Ma, X. (2017). Climatic influence on electricity consumption: The case of Singapore and Hong Kong. *Energy*, 127, 534–543. <https://doi.org/10.1016/j.energy.2017.04.005>
- Aranda, A., Ferreira, G., Mainar-Toledo, M. D., Scarpellini, S., & Llera Sastresa, E. (2012). Multiple regression models to predict the annual energy consumption in the Spanish banking sector. *Energy and Buildings*, 49, 380–387. <https://doi.org/10.1016/j.enbuild.2012.02.040>
- ASHRAE Guideline 14-2014. (2014). *Measurement of energy, demand, and Water savings. ASHRAE Guidel 14-2014.*
- Assareh, E., Behrang, M. A., Assari, M. R., & Ghanbarzadeh, A. (2010). Application of PSO (particle swarm optimization) and GA (genetic algorithm) techniques on demand estimation of oil in Iran. *Energy*, 35, 5223–5229. <https://doi.org/10.1016/j.energy.2010.07.043>
- Belcher, S. E., Hacker, J. N., & Powell, D. S. (2005). Constructing design weather data for future climates. *Building Services Engineering Research & Technology*, 26, 49–61. <https://doi.org/10.1191/0143624405bt1120a>
- Bianco, V., Manca, O., Nardini, S., & Minea, A. A. (2010). Analysis and forecasting of nonresidential electricity consumption in Romania. *Applied Energy*, 87, 3584–3590. <https://doi.org/10.1016/j.apenergy.2010.05.018>
- Carpenter, J., Woodbury, K. A., & O'Neill, Z. (2018). Using change-point and Gaussian process models to create baseline energy models in industrial facilities: A comparison. *Applied Energy*, 213, 415–425. <https://doi.org/10.1016/j.apenergy.2018.01.043>
- Census and Statistics Department of Hong Kong. (2019a). *Energy electricity consumption (Terajoule), Hong Kong*. <https://www.censtatd.gov.hk/hkstat/sub/so90.jsp>
- Census and Statistics Department of Hong Kong. (2019b). *National income and balance of payments, Hong Kong*. <https://www.censtatd.gov.hk/hkstat/sub/sp50.jsp>
- Chabouni, N., Belarbi, Y., & Benhassine, W. (2020). Electricity load dynamics, temperature and seasonality Nexus in Algeria. *Energy*, 200, Article 117513. <https://doi.org/10.1016/j.energy.2020.117513>
- Chan, H. S., & Tong, H. W. (2014). Temperature projection for Hong Kong in the 21st century using CMIP5 models. *28th Guangdong-Hong Kong-Macao Seminar on Meteorological Science and Technology*.
- Chen, G., Zhu, Y., Wiedmann, T., Yao, L., Xu, L., & Wang, Y. (2019). Urban-rural disparities of household energy requirements and influence factors in China: Classification tree models. *Applied Energy*, 250, 1321–1335. <https://doi.org/10.1016/j.apenergy.2019.04.170>
- Cheung, C. S. C., & Hart, M. A. (2014). Climate change and thermal comfort in Hong Kong. *International Journal of Biometeorology*, 58, 137. <https://doi.org/10.1007/s00484-012-0608-9>
- da Silva, F. L. C., Cyrino Oliveira, F. L., & Souza, R. C. (2019). A bottom-up bayesian extension for long term electricity consumption forecasting. *Energy*, 167, 198. <https://doi.org/10.1016/j.energy.2018.10.201>
- Deng, H., Fannon, D., & Eckelman, M. J. (2018). Predictive modeling for US commercial building energy use: A comparison of existing statistical and machine learning algorithms using CBECS microdata. *Energy and Buildings*, 163, 34–43. <https://doi.org/10.1016/j.enbuild.2017.12.031>
- Development Bureau, & Transport and Housing Bureau. (2015). *Energy saving plan for Hong Kong's built environment 2015–2025+*. Environment Bureau.
- Electrical & Mechanical Services Department. (2019). *Hong Kong energy end-use data 2019, Hong Kong*. <https://www.emsd.gov.hk>
- Environment Bureau. (2017). *Hong Kong's climate action plan 2030+*. Hong Kong www.climateready.gov.hk
- Fan, J. L., Hu, J. W., & Zhang, X. (2019). Impacts of climate change on electricity demand in China: An empirical estimation based on panel data. *Energy*, 170, 880–888. <https://doi.org/10.1016/j.energy.2018.12.044>
- Fang, T., & Lahdelma, R. (2016). Evaluation of a multiple linear regression model and SARIMA model in forecasting heat demand for district heating system. *Applied Energy*, 179, 544–552. <https://doi.org/10.1016/j.apenergy.2016.06.133>
- Foucuquier, A., Robert, S., Suard, F., Stéphan, L., & Jay, A. (2013). State of the art in building modelling and energy performances prediction: A review. *Renewable and Sustainable Energy Reviews*, 23, 272–288. <https://doi.org/10.1016/j.rser.2013.03.004>
- Fung, W. Y., Lam, K. S., Hung, W. T., Pang, S. W., & Lee, Y. L. (2006). Impact of urban temperature on energy consumption of Hong Kong. *Energy*, 31, 2623–2637. <https://doi.org/10.1016/j.energy.2005.12.009>
- García-Ascanio, C., & Maté, C. (2010). Electric power demand forecasting using interval time series: A comparison between VAR and iMLP. *Energy Policy*, 38, 715–725. <https://doi.org/10.1016/j.enpol.2009.10.007>
- Gayawan, E., & Ipinoyomi, R. A. (2009). A comparison of Akaike, Schwarz and R square criteria for model selection using some fertility models. *Australian Journal of Basic and Applied Sciences*.
- Ghalekhondabi, I., Ardjmand, E., Weckman, G. R., & Young, W. A. (2017). An overview of energy demand forecasting methods published in 2005–2015. *IEEE Power and Energy Technology Systems Journal*, 8, 411–447. <https://doi.org/10.1007/s12667-016-0203-y>
- Ghods, L., & Kalantar, M. (2011). Different methods of long-term electric load demand forecasting: a comprehensive review. *Iranian Journal of Electrical & Electronic Engineering*, 7, 249.
- Guan, L. (2009). Preparation of future weather data to study the impact of climate change on buildings. *Building and Environment*, 44, 793–800. <https://doi.org/10.1016/j.buildenv.2008.05.021>
- Günay, M. E. (2016). Forecasting annual gross electricity demand by artificial neural networks using predicted values of socio-economic indicators and climatic conditions: Case of Turkey. *Energy Policy*, 90, 92–101. <https://doi.org/10.1016/j.enpol.2015.12.019>
- Hamedmoghadam, H., Joorabloo, N., & Jalili, M. (2018). *Australia's long-term electricity demand forecasting using deep neural networks*. <https://arxiv.org/abs/1801.02148v2>
- Han, J., Kamber, M., & Pei, J. (2012). *Data mining: Concepts and techniques*. <https://doi.org/10.1016/C2009-0-61819-5>
- He, Y., Wang, M., Guang, F., & Zhao, W. (2020). Research on the method of electricity demand analysis and forecasting: The case of China. *Electric Power Systems Research*, 187, Article 106408. <https://doi.org/10.1016/j.epsr.2020.106408>
- Hobbs, B. F. (1999). Analysis of the value for unit commitment of improved load forecasts. *IEEE Trans Power Syst*, 14, 1342–1348. <https://doi.org/10.1109/59.801894>
- Hong Kong Observatory. (2019). *The year's weather - 2018, Hong Kong*. <https://www.weather.gov.hk/wxinfo/pastwx/2018/ywx2018.htm>
- Isaac, M., & van Vuuren, D. P. (2009). Modeling global residential sector energy demand for heating and air conditioning in the context of climate change. *Energy Policy*, 37, 507–521. <https://doi.org/10.1016/j.enpol.2008.09.051>
- James, G., Witten, D., Hastie, T., & Tibshirani, R. (2013). *An introduction to statistical learning with applications in r (older version)*. <https://doi.org/10.1007/978-1-4614-7138-7>
- Jang, Y., Byon, E., Jahani, E., & Cetin, K. (2020). On the long-term density prediction of peak electricity load with demand side management in buildings. *Energy and Buildings*, 228, Article 110450. <https://doi.org/10.1016/j.enbuild.2020.110450>
- Kaboli, S. H. A., Fallahpour, A., Selvaraj, J., & Rahim, N. A. (2017). Long-term electrical energy consumption formulating and forecasting via optimized gene expression programming. *Energy*, 126, 144–164. <https://doi.org/10.1016/j.energy.2017.03.009>
- Kandananon, K. (2011). Forecasting electricity demand in Thailand with an artificial neural network approach. *Energies*, 4, 1246–1257. <https://doi.org/10.3390/en4081246>
- Kankal, M., Akpınar, A., Kömürçü, M. I., & Özşahin, TŞ. (2011). Modeling and forecasting of Turkey's energy consumption using socio-economic and demographic variables. *Applied Energy*, 88, 1927–1939. <https://doi.org/10.1016/j.apenergy.2010.12.005>
- Kavaklioglu, K. (2011). Modeling and prediction of Turkey's electricity consumption using Support Vector Regression. *Applied Energy*, 88, 368–375. <https://doi.org/10.1016/j.apenergy.2010.07.021>
- Kaytez, F., Taplamacioglu, M. C., Cam, E., & Hardalac, F. (2015). Forecasting electricity consumption: A comparison of regression analysis, neural networks and least squares support vector machines. *International Journal of Electrical Power & Energy Systems*, 67, 431–438. <https://doi.org/10.1016/j.ijepes.2014.12.036>
- Khuntia, S. R., Rueda, J. L., & van der Meijden, M. A. M. (2016). Forecasting the load of electrical power systems in mid- and long-term horizons: A review. *IET Generation Transmission & Distribution*, 10, 3971–3977. <https://doi.org/10.1049/iet-gtd.2016.0340>
- Knutti, R., & Jan, S. (2013). Robustness and uncertainties in the new CMIP5 climate model projections. *Nat Clim Change*, 3(4), 369–373. <https://doi.org/10.1038/nclimate1716>
- Kolokotsa, D., & Santamouris, M. (2015). Review of the indoor environmental quality and energy consumption studies for low income households in Europe. *The Science of the Total Environment*, 536, 316–330. <https://doi.org/10.1016/j.scitotenv.2015.07.073>
- Kontokosta, C. E., & Tull, C. (2017). A data-driven predictive model of city-scale energy use in buildings. *Applied Energy*, 197, 303–317. <https://doi.org/10.1016/j.apenergy.2017.04.005>
- Lam, J. C. (1998). Climatic and economic influences on residential electricity consumption. *Energy Conversion and Management*, 39, 623–629. [https://doi.org/10.1016/S0196-8904\(97\)10008-5](https://doi.org/10.1016/S0196-8904(97)10008-5)
- Lam, J. C., Wan, K. K. W., Lam, T. N. T., & Wong, S. L. (2010). An analysis of future building energy use in subtropical Hong Kong. *Energy*, 35, 1482–1490. <https://doi.org/10.1016/j.energy.2009.12.005>
- Lau, K. K. L., Ng, E. Y. Y., Chan, P. W., & Ho, J. C. K. (2017). Near-extreme summer meteorological data set for sub-tropical climates. *Building Services Engineering Research & Technology*, 38, 197–208. <https://doi.org/10.1177/0143624416675390>

- Lee, T. C., Kok, M. H., Chan, K. Y., Kong, H., & June, M. (2010). Climatic influences on the energy consumption in domestic and commercial sectors in Hong Kong. *The 16th Annual International Sustainable Development Research*.
- Li, X. X. (2018). Linking residential electricity consumption and outdoor climate in a tropical city. *Energy*, 157, 734–743. <https://doi.org/10.1016/j.energy.2018.05.192>
- Li, D. H. W., Yang, L., & Lam, J. C. (2012). Impact of climate change on energy use in the built environment in different climate zones - A review. *Energy*, 42, 103–112. <https://doi.org/10.1016/j.energy.2012.03.044>
- Liang, Y., Niu, D., Cao, Y., & Hong, W. C. (2016). Analysis and modeling for China's electricity demand forecasting using a hybrid method based on multiple regression and extreme learning machine: A view from carbon emission. *Energies*, 9, Article 941. <https://doi.org/10.3390/en9110941>
- Lindberg, K. B., Seljom, P., Madsen, H., Fischer, D., & Korpås, M. (2019). Long-term electricity load forecasting: Current and future trends. *Utilities Policy*, 58, 102–119. <https://doi.org/10.1016/j.jup.2019.04.001>
- Liu, S., Kwok, Y. T., Lau, K. K. L., Tong, H. W., Chan, P. W., & Ng, E. (2020). Development and application of future design weather data for evaluating the building thermal-energy performance in subtropical Hong Kong. *Energy and Buildings*, 209, Article 109696. <https://doi.org/10.1016/j.enbuild.2019.109696>
- Liu, S., Kwok, Y. T., Lau, K. K. L., Ouyang, W., & Ng, E. (2020). Effectiveness of passive design strategies in responding to future climate change. For residential buildings in hot and humid Hong Kong. *Energy and Buildings*, 228, Article 110469. <https://doi.org/10.1016/j.enbuild.2020.110469>
- Luk, S. (2005). Electricity tariffs in Hong Kong: What went wrong and what can we do about it? *Energy Policy*, 33, 1085–1093. <https://doi.org/10.1016/j.enpol.2003.11.008>
- Luo, M., Cao, B., Damiens, J., Lin, B., & Zhu, Y. (2015). Evaluating thermal comfort in mixed-mode buildings: A field study in a subtropical climate. *Building and Environment*, 88, 46–54. <https://doi.org/10.1016/j.buildenv.2014.06.019>
- Luo, X. J., Oyedele, L. O., Ajayi, A. O., & Akinade, O. O. (2020). Comparative study of machine learning-based multi-objective prediction framework for multiple building energy loads. *Sustainable Cities and Society*, 61, Article 102283. <https://doi.org/10.1016/j.scs.2020.102283>
- Ma, J., & Cheng, J. C. P. (2016). Identifying the influential features on the regional energy use intensity of residential buildings based on Random Forests. *Applied Energy*, 183, 193–201. <https://doi.org/10.1016/j.apenergy.2016.08.096>
- Mei, H., Li, Y. P., Suo, C., Ma, Y., & Lv, J. (2020). Analyzing the impact of climate change on energy-economy-carbon nexus system in China. *Applied Energy*, 262, Article 114568. <https://doi.org/10.1016/j.apenergy.2020.114568>
- Moazami, A., Nik, V. M., Carlucci, S., & Geving, S. (2019). Impacts of future weather data typology on building energy performance - Investigating long-term patterns of climate change and extreme weather conditions. *Applied Energy*, 238, 696–720. <https://doi.org/10.1016/j.apenergy.2019.01.085>
- Mora, C., Frazier, A. G., Longman, R. J., Dacks, R. S., Walton, M. M., Tong, E. J., et al. (2013). The projected timing of climate departure from recent variability. *Nature*, 502, 183–187. <https://doi.org/10.1038/nature12540>
- Morakinyo, T. E., Ren, C., Shi, Y., Lau, K. K. L., Tong, H. W., Choy, C. W., et al. (2019). Estimates of the impact of extreme heat events on cooling energy demand in Hong Kong. *Renewable Energy*, 142, 73–84. <https://doi.org/10.1016/j.renene.2019.04.077>
- O'Neill, B. C., Krieger, E., Riahi, K., Ebi, K. L., Hallegatte, S., Carter, T. R., et al. (2014). A new scenario framework for climate change research: The concept of shared socioeconomic pathways. *Climatic Change*, 122, 387–400. <https://doi.org/10.1007/s10584-013-0905-2>
- Pérez-García, J., & Moral-Carcedo, J. (2016). Analysis and long term forecasting of electricity demand through a decomposition model: A case study for Spain. *Energy*, 97, 127–143. <https://doi.org/10.1016/j.energy.2015.11.055>
- Peters, G. P., Andrew, R. M., Boden, T., Canadell, J. G., Ciais, P., Le Quéré, C., et al. (2013). The challenge to keep global warming below 2C. *Nature Climate Change*, 3, 4–6. <https://doi.org/10.1038/nclimate1783>
- Pilli-Sihvola, K., Aatola, P., Ollikainen, M., & Tuomenvirta, H. (2010). Climate change and electricity consumption-Witnessing increasing or decreasing use and costs? *Energy Policy*, 38, 2409–2419. <https://doi.org/10.1016/j.enpol.2009.12.033>
- Riahi, K., van Vuuren, D. P., Krieger, E., Edmonds, J., O'Neill, B. C., Fujimori, S., et al. (2017). The shared Socioeconomic Pathways and their energy, land use, and greenhouse gas emissions implications: An overview. *Global Environmental Change*, 42, 153–168. <https://doi.org/10.1016/j.gloenvcha.2016.05.009>
- Robinson, C., Dilkina, B., Hubbs, J., Zhang, W., Guhathakurta, S., Brown, M. A., et al. (2017). Machine learning approaches for estimating commercial building energy consumption. *Applied Energy*, 208, 889–904. <https://doi.org/10.1016/j.apenergy.2017.09.060>
- Sangrody, H., Zhou, N., & Tutun, S. (2018). Long term forecasting using machine learning methods. *2018 IEEE Power and Energy Conference at Illinois*. <https://doi.org/10.1109/PECI.2018.8334980>
- Santamouris, M. (2013). Using cool pavements as a mitigation strategy to fight urban heat island - A review of the actual developments. *Renewable and Sustainable Energy Reviews*, 26, 224–240. <https://doi.org/10.1016/j.rser.2013.05.047>
- Santamouris, M. (2016). Cooling the buildings-past, present and future. *Energy and Buildings*, 128, 617–638. <https://doi.org/10.1016/j.enbuild.2016.07.034>
- Seyedzadeh, S., Pour Rahimian, F., Rastogi, P., & Glesk, I. (2019). Tuning machine learning models for prediction of building energy loads. *Sustainable Cities and Society*, 47, Article 101484. <https://doi.org/10.1016/j.scs.2019.101484>
- Shao, M., Wang, X., Bu, Z., Chen, X., & Wang, Y. (2020). Prediction of energy consumption in hotel buildings via support vector machines. *Sustainable Cities and Society*, 57, Article 102128. <https://doi.org/10.1016/j.scs.2020.102128>
- Taylor, K. E., Stouffer, R. J., & Meehl, G. A. (2012). An overview of CMIP5 and the experiment design. *Bulletin of the American Meteorological Society*, 93, 485–498. <https://doi.org/10.1175/BAMS-D-11-00094.1>
- Toktarova, A., Gruber, L., Hlusiak, M., Bogdanov, D., & Breyer, C. (2019). Long term load projection in high resolution for all countries globally. *International Journal of Electrical Power & Energy Systems*, 111, 160–181. <https://doi.org/10.1016/j.ijepes.2019.03.055>
- Tong, H. W., Wong, C. P., & Lee, S. M. (2017). Projection of wet-bulb temperature for Hong Kong in the 21st century using CMIP5 data. In *The 31st Guangdong - Hong Kong - Macao Seminar on Meteorological Science and Technology and The 22nd Guangdong - Hong Kong - Macao Meeting on Cooperation in Meteorological Operations*.
- Torrini, F. C., Souza, R. C., Cyrino Oliveira, F. L., & Moreira Pessanha, J. F. (2016). Long term electricity consumption forecast in Brazil: A fuzzy logic approach. *Socio-economic Planning Sciences*, 54, 18–27. <https://doi.org/10.1016/j.seps.2015.12.002>
- Touzani, S., Granderson, J., & Fernandes, S. (2018). Gradient boosting machine for modeling the energy consumption of commercial buildings. *Energy and Buildings*. <https://doi.org/10.1016/j.enbuild.2017.11.039>
- Trotter, I. M., Bolkesjø, T. F., Féres, J. G., & Hollanda, L. (2016). Climate change and electricity demand in Brazil: A stochastic approach. *Energy*, 102, 596–604. <https://doi.org/10.1016/j.energy.2016.02.120>
- Troup, L., Eckelman, M. J., & Fannon, D. (2019). Simulating future energy consumption in office buildings using an ensemble of morphed climate data. *Applied Energy*, 255, Article 113821. <https://doi.org/10.1016/j.apenergy.2019.113821>
- Vu, D. H., Muttaqi, K. M., & Agalgaonkar, A. P. (2015). A variance inflation factor and backward elimination based robust regression model for forecasting monthly electricity demand using climatic variables. *Applied Energy*, 140, 385–394. <https://doi.org/10.1016/j.apenergy.2014.12.011>
- Wan, K. S. Y., & Yik, F. W. H. (2004). Building design and energy end-use characteristics of high-rise residential buildings in Hong Kong. *Applied Energy*, 78, 19–36. [https://doi.org/10.1016/S0306-2619\(03\)00103-X](https://doi.org/10.1016/S0306-2619(03)00103-X)
- Wan, K. K. W., Li, D. H. W., & Lam, J. C. (2011). Assessment of climate change impact on building energy use and mitigation measures in subtropical climates. *Energy*, 36, 1404–1414. <https://doi.org/10.1016/j.energy.2011.01.033>
- Wan, K. K. W., Li, D. H. W., Liu, D., & Lam, J. C. (2011). Future trends of building heating and cooling loads and energy consumption in different climates. *Building and Environment*, 46, 223–234. <https://doi.org/10.1016/j.buildenv.2010.07.016>
- Xia, C., Wang, J., & McMenemy, K. (2010). Short, medium and long term load forecasting model and virtual load forecaster based on radial basis function neural networks. *Int J Electr Power Energy Syst*, 32, 743–750. <https://doi.org/10.1016/j.ijepes.2010.01.009>
- Yang, L., Yan, H., & Lam, J. C. (2014). Thermal comfort and building energy consumption implications - A review. *Applied Energy*, 115, 164–173. <https://doi.org/10.1016/j.apenergy.2013.10.062>
- Yang, Y., Li, S., Li, W., & Qu, M. (2018). Power load probability density forecasting using Gaussian process quantile regression. *Applied Energy*, 213, 499–509. <https://doi.org/10.1016/j.apenergy.2017.11.035>
- You, Q., Fraedrich, K., Sielmann, F., Min, J., Kang, S., Ji, Z., et al. (2014). Present and projected degree days in China from observation, reanalysis and simulations. *Climate Dynamics*, 43, 1449–1462. <https://doi.org/10.1007/s00382-013-1960-0>
- Yu, Z., Haghghat, F., Fung, B. C. M., & Yoshino, H. (2010). A decision tree method for building energy demand modeling. *Energy and Buildings*, 42, 1637–1646. <https://doi.org/10.1016/j.enbuild.2010.04.006>
- Yu, S., Wei, Y. M., & Wang, K. (2012). A PSO-GA optimal model to estimate primary energy demand of China. *Energy Policy*, 42, 329–340. <https://doi.org/10.1016/j.enpol.2011.11.090>
- Zhai, Z. J., & Helman, J. M. (2019). Implications of climate changes to building energy and design. *Sustainable Cities and Society*, 44, 511–519. <https://doi.org/10.1016/j.scs.2018.10.043>
- Zheng, S., Huang, G., Zhou, X., & Zhu, X. (2020). Climate-change impacts on electricity demands at a metropolitan scale: A case study of Guangzhou, China. *Applied Energy*, 261, Article 114295. <https://doi.org/10.1016/j.apenergy.2019.114295>
- Zhu, M., Pan, Y., Huang, Z., & Xu, P. (2016). An alternative method to predict future weather data for building energy demand simulation under global climate change. *Energy and Buildings*, 113, 74–86. <https://doi.org/10.1016/j.enbuild.2015.12.020>
- Zhong, H., Wang, J., Jia, H., Mu, Y., & Lv, S. (2019). Vector field-based support vector regression for building energy consumption prediction. *Applied Energy*, 242, 403–414. <https://doi.org/10.1016/j.apenergy.2019.03.078>